Published in final edited form as:
Compr Physiol. 2013 April ; 3(2): 667–692. doi:10.1002/cphy.c110014.

Phenomics of Cardiac Chloride Channels

Dayue Darrel Duan[*,1]
[1]The Laboratory of Cardiovascular Phenomics, Department of Pharmacology, University of Nevada, School of Medicine, Reno, Nevada

Abstract

Forward genetic studies have identified several chloride (Cl^-) channel genes, including *CFTR*, *ClC-2*, *ClC-3*, *CLCA*, *Bestrophin*, and *Ano1*, in the heart. Recent reverse genetic studies using gene targeting and transgenic techniques to delineate the functional role of cardiac Cl^- channels have shown that Cl^- channels may contribute to cardiac arrhythmogenesis, myocardial hypertrophy and heart failure, and cardioprotection against ischemia reperfusion. The study of physiological or pathophysiological phenotypes of cardiac Cl^- channels, however, is complicated by the compensatory changes in the animals in response to the targeted genetic manipulation. Alternatively, tissue-specific conditional or inducible knockout or knockin animal models may be more valuable in the phenotypic studies of specific Cl^- channels by limiting the effect of compensation on the phenotype. The integrated function of Cl^- channels may involve multiprotein complexes of the Cl^- channel subproteome. Similar phenotypes can be attained from alternative protein pathways within cellular networks, which are influenced by genetic and environmental factors. The phenomics approach, which characterizes phenotypes as a whole phenome and systematically studies the molecular changes that give rise to particular phenotypes achieved by modifying the genotype under the scope of genome/proteome/phenome, may provide more complete understanding of the integrated function of each cardiac Cl^- channel in the context of health and disease.

Introduction

The discovery of a cyclic adenosine monophosphate (cAMP)-activated Cl^- current in rabbit ventricular myocytes by Harvey and Hume (81) and in guinea pig heart by Bahinski et al. (1) in 1989 ushered the new era of Cl^- channel studies in the heart. Patch-clamp studies have described a variety of Cl^- channels with different single-channel conductance, anion selectivity, and mechanism of regulation in both plasma membrane and intracellular organelles of cardiac cells isolated from different regions of the heart and in different species (Fig. 1) (60, 90, 172). The biophysical, pharmacological, and molecular properties of Cl^- channels in the heart have been well characterized and summarized in several excellent review articles (4, 60, 74, 80, 85, 90). Forward genetic approaches have been used to identify the genes responsible for the Cl^- currents found in the heart. At the molecular level, all cardiac Cl^- channels described so far may fall into the following Cl^- channel gene families: (i) the cystic fibrosis transmembrane conductance regulator (*CFTR*), which is a member of the adenosine triphosphate-binding cassette (ABC) transporter superfamily and may be responsible for the Cl^- currents activated by protein kinase A (PKA) ($I_{Cl,PKA}$) (1, 81, 120), protein kinase C (PKC) ($I_{Cl,PKC}$) (33, 160), and extracellular ATP ($I_{Cl,ATP}$) (57, 107, 173); (ii) *ClC-2*, which is a member of the ClC voltage-gated Cl^- channel superfamily and may be responsible for the inwardly rectifying Cl^- current ($I_{Cl,ir}$) activated by

[*]Correspondence to dduan@medicine.nevada.edu.

hyperpolarization and cell swelling (56); (iii) *ClC-3*, which is also a member of the ClC voltage-gated Cl^- channel superfamily and may be responsible for the volume-regulated outwardly rectifying Cl^- current ($I_{Cl,vol}$), including the basally activated ($I_{Cl,b}$) (50), and swelling-activated ($I_{Cl,swell}$) components (49–52, 54, 55, 58, 83, 161, 174); (iv) Ano1, (or TMEM16A), which is a novel candidate gene for the Ca^{2+}-activated Cl^- current ($I_{Cl,Ca}$) (21,138,175).; (v) *CLCA-1*, which was thought to be responsible for $I_{Cl,Ca}$ (15,34,171); and (vi) *Bestrophin*, also a candidate for $I_{Cl,Ca}$ (79). In addition, it has been recently demonstrated by several groups that the voltage-dependent anion channel 1 (VDAC1), which is predominantly expressed in the outer membrane of mitochondrion, is also expressed in the sarcolemmal membrane (2, 63, 166). A novel Cl^- current activated by extracellular acidosis ($I_{Cl,acid}$) has also been observed in cardiac myocytes but the molecular identity for $I_{Cl,acid}$ is currently not known (Fig. 1).

Previous *in vitro* experimental evidence has suggested that Cl^- channels in the plasma membrane may be involved in the regulation of a large repertoire of cellular functions, including cellular excitability, intracellular organelle acidification, cell volume homeostasis, cell migration, proliferation, differentiation, and apoptosis (4, 90, 105, 126). The understanding of Cl^- channel function in cardiac physiology and pathophysiology, however, has been hampered by the concomitant expression of several types of Cl^- channels in the same cardiac cell and by the lack of specific pharmacological tools to effectively separate the individual Cl^- channels. For example, most studies that have examined the contribution of Cl^- currents to the cardiac action potential and arrhythmias have relied on Cl^- channel blockers and anion substitution experiments. The pharmacological specificity of many of these Cl^- channel blockers can be problematic, and anion substitution, in addition to altering anion movement through channels, can have other unpredictable side effects on other transport proteins and signaling pathways (64, 121).

The recent identification of molecular entities responsible for cardiac Cl^- channels (60, 90) has made it possible to combine gene-targeting techniques with electrophysiology, molecular biology, and functional genomics and proteomics in the study of cardiac Cl^- channels. Studies from transgenic and gene knockout mice have shown that Cl^- channels may be important in arrhythmogenesis, myocardial hypertrophy, heart failure, and cardioprotection against ischemia and reperfusion. Recent evidence has also demonstrated, however, that the study of physiological or pathophysiological phenotypes of cardiac Cl^- channels may be complicated by the compensatory changes in the animals in response to the targeted genetic manipulation (165, 174). To limit the effect of up-regulation or developmental compensation on the phenotype of manipulated genes, tissue-specific conditional or inducible knockout or knockin animal models have been used as alternative approaches in the phenotypic studies of specific Cl^- channel genes. In addition, recent evidence indicates that proteins do not act as single players but as part of functional complexes whose composition, subcellular localization, and interaction orchestrate their biological role under different conditions. In addition, the integrated function of Cl^- channels may involve multiple proteins of the Cl^- channel subproteome and interactome. Similar phenotypes can be attained from alternative protein pathways within the cellular network. Therefore, the genotype-phenotype relationship of integrated Cl^- channels and the molecular changes that give rise to particular phenotypes achieved by modifying the genotype (Cl^- channel gene knockouts or knockins) should be studied systematically under the scope of genome, proteome, and phenome. The phenomics approach, which characterizes phenotypes as a whole phenome, may provide more complete understanding of the functional role of each cardiac Cl^- channel under normal and diseased conditions.

This article will highlight the major findings and recent advances in phenotypic studies of cardiac Cl^- channels and discuss the possible uses of phenomics as an integrative approach to the systematic and meticulous understanding of Cl^- channel function in the heart.

Phenotypic Study of Cardiac Channels

Phenotypic study of cardiac CFTR channels

Functional role of CFTR in cardiac electrophysiology and arrythmogenesis—

Early studies of intracellular Cl^- activity (a^i_{Cl}) in cardiac myocytes using ion-selective microelectrode estimated an intracellular Cl^- concentration ($[Cl^-]_i$) of 10 to 20 mmol/L under normal physiological conditions (5, 20, 144, 151). With an extracellular Cl^- concentration ($[Cl^-]_o$) of 145 mmol/L, therefore, the equilibrium potential for Cl^- (E_{Cl}) is within a membrane potential range (usually −65 to −40 mV) that is more positive than the resting membrane potential and can be either negative or positive to the actual membrane potential during the normal cardiac cycle. Thus, compared with cationic channels, cardiac Cl^- channels have the unique ability to generate both inward and outward currents and cause both depolarization and repolarization during the action potential. Therefore, activation of Cl^- channels may produce significant effects on cardiac action potential characteristics (Fig. 2) and pacemaker activity (Fig. 3). The degree to which activation of Cl^- currents depolarizes the resting membrane or accelerates the repolarization of action potential depends critically on the actual value of E_{Cl} and the magnitude of the Cl^- conductance relative to the total membrane conductance.

Under basal physiological conditions CFTR channels are mostly closed and are activated only when the intracellular PKA- and PKC-dependent phosphorylation activity is increased (57, 70, 90). The activation of CFTR Cl^- channels in the heart will result in outwardly rectifying currents because the transmembrane Cl^- gradient is asymmetrical. This will have more significant effects at positive potentials to accelerate repolarization and cause a shortening of the action potential duration (APD) compared with smaller depolarizing effects at negative potentials near the resting membrane potential (Fig. 2, top panel). Thus, activation of CFTR channels will result in a shortening of Q-T interval (Fig. 2, bottom panel). The ability of Cl^- current activation to depolarize cardiac cells is also opposed by the presence of a large background K^+ conductance that normally controls the resting membrane potential. Both abbreviation of APD and depolarization of E_m upon activation of Cl^- channels may induce early afterdepolarization (EAD) and play a role in arrhythmogenesis under pathological conditions.

Telemetry electrocardiogram (ECG) recordings revealed no significant difference in ECG parameters between $CFTR^{-/-}$ mice and their wild-type (WT) littermates (Xiang et al., unpublished observations), which is consistent with the low basal activity of CFTR channels in the heart. A major physiological role of activation of CFTR may be to prevent excessive APD prolongation and protect the heart against the development of EAD and triggered activity caused by β-adrenergic stimulation of Ca^{2+} channels (Fig. 2). It is well-established that APD prolongation favors EADs by allowing recovery of inward currents and, conversely, shortening of APD makes it more difficult to induce EADs. EADs arising from phase 2 and 3 underlie focal triggered tachyarrhythmias and repolarization abnormalities, which contribute to cardiac sudden death. Therefore, activation of CFTR channels should protect against focal triggered arrhythmias. However, when background K^+ conductance is reduced in the case of myocardial hypokalemia, activation of CFTR channels will cause significant membrane depolarization and induce abnormal automaticity. These predicted effects of CFTR channel activation on APD and automaticity have been verified experimentally by manipulations of the Cl^- gradient or the use of Cl^- channel blockers (82,85). Histamine was found to activate CFTR channels in ventricular myocytes and induce

oscillatory activity and abnormal impulses in the heart, although the contribution of CFTR channels to these arrhythmogenic activities has not been further explored. It has been shown that activation of CFTR channels contributes to hypoxia-induced shortening in APD (133). Activation of CFTR channels may accelerate the development of reentry due to shortening of APD and refractoriness and a decrease in conduction velocity caused by a slight depolarization of diastolic potential leading to Na^+ channel inactivation.

Functional role of CFTR in myocardial hypertrophy and heart failure— Remodeling of CFTR channels has been observed in myocardial hypertrophy and heart failure. Using *in situ* mRNA hybridization in a combined pressure and volume overload model of heart failure in the rabbit, Wong et al. found that the normal epicardial to endocardial gradient of CFTR mRNA expression is reversed due to a significant decrease in epicardial expression of CFTR mRNA in the rabbit left ventricle (164). A posttranslational change in CFTR expression could be responsible for this phenomenon (39). The loss of the normal transmural gradient of repolarizing ion channels is likely to contribute to instability of repolarization in the hypertrophied heart and hence increased risk of cardiac arrhythmias in patients with heart failure. A very recent study in human failing heart found that the expression of the mature CFTR protein decreased significantly to 52% of CFTR levels in non-failing controls (141). Interestingly, it was reported recently that a pediatric patient who died of heart failure with significant myocardial lesion was retrospectively diagnosed as cystic fibrosis only after the histological examination of a liver biopsy (32). The exact functional and clinical significance of the changes in CFTR expression during hypertrophy and heart failure is currently not clear and merits further study.

CFTR channels and cardioprotection against ischemia/reperfusion damage— We have previously found that targeted inactivation of the CFTR gene abolished the protective effects of ischemic preconditioning on cardiac function and myocardium injury against sustained ischemia in isolated mouse heart (Fig. 3) (23). Our preliminary *in vivo* studies using both WT and CFTR knockout mice also demonstrated that CFTR is an important mediator in both early and late ischemic preconditioning in the heart (176). We also found that the CFTR channels may play a key role in the postconditioning induced cardioprotection in mouse heart (167).

CFTR interactome and its versatile physiological functions—While CFTR is best characterized as a Cl^- channel, considerable evidence in noncardiac cells have demonstrated that CFTR is also a channel for other physiologically important anions such as the reduced form of glutathione (gamma-glutamyl-cysteinyl-glycine) (71,99,109), ATP (131,134,146), and HCO_3^- (116). CFTR has been found to transport other molecules such as sphingosine-1-phosphate (11) and to be involved in the release of cytokines (158) and in the regulation of activities of many other ion channels and transporters such as epithelial Na^+ channels (103, 104) and Ca^{2+}- and volume-activated Cl^- channels (103). The integrated versatile functions and complex regulation of the CFTR channels may be concerted by a number of proteins in the CFTR interactome (Fig. 4) (162), which may include the chaperones that facilitate the processing and trafficking of CFTR protein, the proteins that control CFTR activity through signaling mechanisms, and other proteins such as ion channels and transporters that CFTR regulates (76,77,103,104,122,140,162).

Phenotypic study of cardiac ClC-3 channels

Functional role of volume-regulated Cl^- channels and ClC-3 in electrophysiology and arrythmogenesis—The current through the volume-regulated Cl^- channels (VRCCs) under basal or isotonic conditions ($I_{Cl,b}$) is small (50,52,142), but can be further activated by stretching of the cell membrane by inflation (47) or direct mechanical

stretch of membrane β_1-integrin (17) and/or cell swelling induced by exposure to hypoosmotic solutions (47,49,55,142). Because of its stronger outwardly rectifying property activation of VRCCs is expected to produce depolarization of the resting membrane potential and more significant APD shortening than activation of CFTR channels (Fig. 2) (47, 52, 54, 150). Shortening of APD and, therefore, the effective refractory period, reduces the length of the conducting pathway needed to sustain reentry (wavelength). In principle, this favors the development of atrial or ventricular fibrillation, which depends on the presence of multiple reentrant circuits or rotating spiral waves. Myocardial cells swell during hypoxia and ischemia, and the washout of hyperosmotic extracellular fluid after reperfusion induces further cell swelling. Therefore, activation of VRCCs may also contribute to hypoxia, ischemia, and reperfusion induced shortening of APD and arrhythmias (4,47,150). $I_{Cl,swell}$ also may slow or enhance the conduction of early extrasystoles, depending on the timing. In guinea-pig heart, hypoosmotic solution shortened APDs and increased APD gradients between right and left ventricles (25). In ventricular fibrillation (VF) induced by burst stimulation of isolated guinea-pig heart, switching to hypoosmotic solution increased VF frequencies, transforming complex fast Fourier transformation spectra to a single dominant high frequency on the left but not the right ventricle (25). Perfusion with the VRCC blocker indanyloxyacetic acid-94 reversed organized VF to complex VF with lower frequencies, indicating that VRCC underlies the changes in VF dynamics. Consistent with this interpretation, ClC-3 channel protein expression is 27% greater on left than right ventricles, and computer simulations showed that insertion of $I_{Cl,vol}$ transformed complex VF to a stable spiral. Therefore, activation of $I_{Cl,vol}$ has a major impact on VF dynamics by transforming random multiple wavelets to a highly organized VF with a single dominant frequency (25). These observations have significant clinical relevance and merit further confirmation from *in vivo* studies.

It has been shown that mechanical stretching or dilation of the atrial myocardium is able to cause arrhythmias. Since $I_{Cl,swell}$ was also found in sino-atrial (S-A) nodal cells, VRCCs may serve as a mediator of mechanotransduction and play a significant role in the pacemaker function if they act as the stretch activated channels in these cells (4, 78). Baumgarten's laboratory has demonstrated that $I_{Cl,swell}$ in ventricular myocytes can be directly activated by mechanical stretch through selectively stretching β1-integrins with mAb-coated magnetic beads (4,17,18). Although it has been suggested that stretch and swelling activate the same anion channel in some noncardiac cells, further study is needed to determine whether this is true in cardiac myocytes.

In the case of myocardial hypertrophy and heart failure, ionic remodeling is one of the major features of pathophysiological changes (148). It has been found that the current densities and molecular expression of several major repolarizing K^+ channels (such as Kv4x) are significantly reduced, which may be responsible for the prolongation of APD and development of EAD (148). However, under these conditions, $I_{Cl,vol}$ is constitutively active (31). The persistent activation of $I_{Cl,vol}$ may limit the APD prolongation and make it more difficult to elicit EAD. Indeed, in myocytes from failing hearts, blocking $I_{Cl,vol}$ by tamoxifen significantly prolonged APD and decreased the depolarizing current required to elicit EAD by about 50%. And hyperosmotic cell shrinkage, which also inhibits $I_{Cl,vol}$, was almost equivalent to the effect of tamoxifen on APD and EAD in these myocytes (4).

Therefore, the consequences of activation of $I_{Cl,vol}$ are very complex. It may be detrimental, beneficial, or both simultaneously in different parts of the heart, depending on environmental influences.

Functional role of $I_{Cl,swell}$ and ClC-3 in IPC—It has been reported that the block of $I_{Cl,swell}$ in rabbit cardiac myocytes inhibits preconditioning by brief ischemia, hypoosmotic

stress (42,43) and adenosine receptor agonists (3). These studies were solely based on the use of several Cl^- channel blockers, such as anthracene-9-carboxylic acid and 4-acetamide-4′-isothiocyanatostilbene-2,2′-disulfonic acid. As mentioned above, these pharmacological tools lack specificity to a particular Cl^- channel in the heart and may also act on other ion channels or transporters. Therefore, it has been very difficult to confirm the causal role of $I_{Cl,swell}$ in IPC (84). To specifically test whether the VRCCs are indeed involved in IPC, we have recently established *in vitro* and *in vivo* IPC models in *ClCn3*$^{-/-}$ mice. Our preliminary results indicate that targeted inactivation of *ClC-3* gene prevented protective effects of late IPC but not of early IPC, suggesting that $I_{Cl,swell}$ may contribute differently to early and late IPC (12, 13). The underlying mechanisms for these differential effects are currently unknown. Recent reports, however, suggest that $I_{Cl,swell}$ and ClC-3 might play an important role in apoptosis (74) and inflammation (159). Cl^- channel blockers 4,4′-diisothiocyanato-stilbene-2,2′-disulphonic acid and natriuretic peptide B were as potent as a broad-spectrum caspase inhibitor in preventing apoptosis and elevation of caspase-3 activity and improved cardiac contractile function after ischemia and *in vivo* reperfusion (117). Transgenic mice overexpressing Bcl-2 in the heart had significantly smaller infarct size and reduced apoptosis of myocytes after ischemia and reperfusion (24). It has been shown that Bcl-2 induces up-regulation of $I_{Cl,vol}$ by enhancing ClC-3 expression in human prostate cancer epithelial cells (106). Cell shrinkage is an integral part of apoptosis, suggesting that $I_{Cl,vol}$ and ClC-3 might be intimately linked to apoptotic events through regulation of cell volume homeostasis (74,106,163).

Functional role of $I_{Cl,swell}$ and ClC-3 in myocardial hypertrophy and heart failure—$I_{Cl,swell}$ is persistently activated in ventricular myocytes from a canine pacing-induced dilated cardiomyopathy model (31). Using the perforated patch-clamp technique, Clemo et al. found that, even in isotonic solutions, a large 9AC-sensitive, outwardly rectifying Cl^- current was recorded in failing cardiac myocytes but not in normal cardiac myocytes. Graded hypotonic cell swelling (90%–60% hypotonic) failed to activate additional current while graded hypertonic cell shrinkage caused an inhibition of the “basal” Cl^- current in failing myocytes. Moreover, the maximum current density of the $I_{Cl,swell}$ in failing myocytes was about 40% greater than that in osmotically swollen normal myocytes. Constitutive activation of $I_{Cl,swell}$ is also observed in several other animal models of heart failure, such as a rabbit aortic regurgitation model of dilated cardiomyopathy (29,30), a dog model of heart failure caused by myocardial infarction (31), and a mouse model of myocardial hypertrophy by aorta binding (53). In human atrial myocytes obtained from patients with right atrial enlargement and/or elevated left ventricular end-diastolic pressure, a tamoxifen sensitive $I_{Cl,swell}$ was also found to be persistently activated (129). Therefore, it is possible that persistent activation of $I_{Cl,swell}$ is a common response of cardiac myocytes to hypertrophy or heart failure-induced remodeling.

The mechanism for persistent activation of $I_{Cl,swell}$ in hypertrophied or failing cardiac myocytes is still not clear. Perhaps the increase in cell volume caused by hypertrophy and the stretch of cell membrane caused by dilation are both involved in the activation of $I_{Cl,swell}$. Alternatively, the persistent activation of $I_{Cl,swell}$ may be caused by signaling cascades activated during hypertrophy independent of changes in cell length and volume, or both. It has been reported that cell swelling and membrane stretch may activate Cl^- channels through a common or similar signaling cascade (132). $I_{Cl,swell}$ could be activated by direct stretch of β1-integrin through focal adhesion kinase (FAK) and/or Src (17). Mechanical stretch of myocytes also releases angiotensin II (AngII), which binds to AT1 receptors (AT1R) and stimulates FAK and Src in an autocrineparacrine loop. A recent study by Browe and Baumgarten suggests that the stretch of β1-integrin in cardiac myocytes activates $I_{Cl,swell}$ by activating AT1R and NADPH oxidase (Nox) and, thereby, producing reactive oxygen species (ROS). In addition, NADPH oxidase may be intimately coupled to the

channel responsible for $I_{Cl,swell}$, providing a second regulatory pathway for this channel through membrane stretch or oxidative stress (18). Recently, Baumgarten's laboratory further characterized the regulation of $I_{Cl,swell}$ by endothelin-1 (ET-1)-mediated signaling pathway and found that ET_A receptors were downstream effectors when $I_{Cl,swell}$ was elicited by osmotic swelling or AngII (41). $I_{Cl,swell}$ could be also elicited by ET-1 via ET_A receptors-mediated ROS production by Nox and mitochondria under isosmotic conditions in both atrial and ventricular myocytes (Fig. 5) (41). In some instances mitochondrial ROS turns on VRAC without the involvement of NOX (41). These findings are very important for further understanding of the mechanism for hypertrophy activation of $I_{Cl,swell}$ and ClC-3 channels and their relationship to hypertrophy and heart failure as it is very well known that Ang II plays a crucial role in the remodeling of the heart during myocardial hypertrophy and heart failure (40). Interestingly, Miller Jr. and colleagues recently found that Cl^- channel inhibitors and knockout of ClC-3 abolish cytokine-induced generation of ROS in endosomes and ROS-dependent nuclear factor κB activation in vascular smooth muscle cells (115), suggesting a potential close interaction between NADPH oxidase and ClC-3. In human corneal keratocytes and human fetal lung fibroblasts, ClC-3 knockdown by a short hairpin RNA (shRNA) significantly decreased VRCC and lysophosphatidic acid (LPA)-activated Cl^- current ($I_{Cl,LPA}$) in the presence of transforming growth factor-β1 (TGF-β1) compared with controls, whereas ClC-3 overexpression resulted in increased $I_{Cl,LPA}$ in the absence of TGF-β1 (177). ClC-3 knockdown also resulted in a reduction of α-smooth muscle actin (α-SMA) protein levels in the presence of TGF-β1, whereas ClC-3 overexpression increased α-SMA protein expression in the absence of TGF-β1. In addition, keratocytes transfected with ClC-3 shRNA had a significantly blunted regulatory volume decrease (RVD) response following hyposmotic stimulation compared with controls. These data not only confirm that ClC-3 is important in VRCC function and cell volume regulation but also provide new insight into the mechanism for the ClC-3-mediated fibroblast-to-myofibroblast transition (177).

The functional and clinical significance of VRCCs in the hypertrophied and dilated heart is currently unknown. Using a mouse aortic binding model of myocardial hypertrophy, we have found that globally targeted disruption of *ClC-3* gene (*ClCn3*$^{-/-}$) accelerated the development of myocardial hypertrophy and the discompensatory process (Fig. 6) (59), suggesting that activation of $I_{Cl,vol}$ might be important in the adaptive remodeling of the heart during pressure overload (111). Interestingly, heart failure was found to be accompanied by a reduced $I_{Cl,vol}$ density in rabbit cardiac myocytes (149).

Recent accumulating evidence suggests an important role of ClC-3 and VRCCs in the regulation of cell proliferation induced by hypertrophic alternations in cell volume. Static pressure increased VRCCs and ClC-3 expression and promoted rat aortic vascular smooth muscle cells (VSMCs) proliferation and cell-cycle progression. Inhibition of VRCCs with pharmacological blocker diphenyleneiodonium (DPI) or knockdown of ClC-3 with ClC-3 antisense oligonucleotide dramatically inhibited pressure evoked cell proliferation and cell-cycle progression of rat aortic SMCs (74). These data suggest that ClC-3 and VRCCs may play a critical role in static pressure-induced cell proliferation and cell-cycle progression. Since arterial SMC proliferation is a key event in the development of hypertension-associated vascular disease, ClC-3 and VRCCs may be of unique therapeutic importance for treatment of hypertension-associated vascular complications. It is interesting that DPI has frequently been used to inhibit ROS production mediated by flavoenzymes, particularly NAD(P)H oxidase. DPI also inhibits production of superoxide and H_2O_2 by mitochondria (108). Therefore, DPI inhibition of VRCCs and cell proliferation may not be due to direct blockade of VRCCs.

Recent studies have demonstrated that statins are effective in attenuating vascular remodeling although the underlying mechanisms are still not determined. Liu et al. (112) used integrated, multiple approaches and performed a thorough investigation on the effects of simvastatin on the hypertension induced cerebrovascular remodeling and VRCCs in basilar smooth muscle cells (BASMCs). They first demonstrated that simvastatin improved the hypertension-caused cerebrovascular remodeling in 2-k,2-c renal hypertensive rats. Then they used cultured rat BASMCs to further study the effects of simvastatin on cell proliferation and the whole-cell VRCC current and volume-regulated Cl^- movement. They found that simvastatin inhibited cell proliferation and also the volume-regulated chloride movement and VRCCs which could be abolished by pretreatment of the cells with mevolonate or geranylgeranyl pyrophosphate. In addition, they found that both Rho A inhibitor C3 exoenzyme and Rho kinase inhibitor Y-27632 reduced the cell proliferation and inhibited the volume-regulated chloride channel. Then the authors went on to examine the expression of *ClC-3* gene in vascular smooth muscles and many other cell types in the basilar arteries; they found the expression of ClC-3 was increased during hypertension and simvastatin treatment reduced the upregualtion of ClC-3 expression. Finally, the authors used a gain-of-function approach to examine whether ClC-3 overexpression would antagonize the inhibitory effect of simvastatin on cell proliferation. Indeed they found that increased ClC-3 activity diminished the inhibitory effect of simvastatin on cell proliferation. A positive correlation between cell proliferation and activation of the ClC-3 channels was revealed. Therefore, this study provided novel and convincing experimental evidence that simvastatin improves cerebrovascular remodeling in 2-k,2-c hypertensive rat through inhibition of the vascular SMC proliferation by suppression of volume-regulated ClC-3 channels. These results provided novel mechanistic insight into the beneficial effects of statins in the treatment of hypertension and stroke.

In addition to its important role in cell volume regulation, ClC-3 may also regulate the redox-signaling pathway through interaction with Nox and/or transport of superoxide to improve myocyte viability against oxidative damage (115). It has been reported that activation of ClC-3 may improve the resistance of vascular SMCs to ROS in an environment of elevated inflammatory cytokines in hypertensive pulmonary arteries [see recent reviews by Hume et al. (91)]. ROS has been implicated in cellular signaling processes as well as a cause of oxidative stress-induced cell proliferation (92). One of the major sources of ROS in the vasculature is through one or more isoforms of the phagocytic enzyme NADPH oxidase, a membrane-localized protein that generates the superoxide (O_2^-) anion on the extracellular surface of the plasma membrane (Fig. 7) (59).

As a charged and short-lived anion, it is believed that O_2^- flux is insufficient to initiate intracellular signaling due to the combination of poor permeability through the phospholipid bilayer and a rapid dismutation to its uncharged and more stable derivative, hydrogen peroxide. Recent studies have also shown that ClC-3 may also function as an antiapoptotic mechanism through regulation of cell volume and intracellular pH; and as a regulator of other transport functions involved in the etiology of hypertension (Fig. 7).

Whether statins' beneficial effects could be attributed also to their effects on these cellular functions of ClC-3 in cerebrovascular SMCs during hypertension is still an unanswered question. Nevertheless, regulation of ClC-3 functions in the cardiovascular system is emerging as a novel and important mechanism for the structural remodeling of the vasculature and may provide a novel therapeutic approach for the treatment of many vascular diseases such as hypertension and stroke.

Findings from ClC-3 knockout and transgenic mice—To understand the molecular changes in cardiac function that accompany the knockout of the *Clcn3* gene, we examined

gene and protein expression profiles from *ClCn3*$^{-/-}$ and *ClCn3*$^{+/+}$ mouse heart. Overall 150 genes and 35 proteins are expressed differentially in the heart of the *ClCn3*$^{-/-}$ mouse model compared to those of control *ClCn3*$^{+/+}$ mice (174). Expression of ClC-2 and ClC-1 channels is increased five-fold and fourfold, respectively, while the expression of some cytoskeleton proteins and PKC_{δ} is decreased by more than twofold. To further test the possibility that targeted inactivation of the *Clcn3* gene using a conventional murine global knockout approach might result in compensatory changes in expression of other membrane proteins in cells from *Clcn3*$^{-/-}$ mice, cardiac membrane proteins were isolated from *Clcn3*$^{+/+}$ and *Clcn3*$^{-/-}$ mice and analyzed using two-dimensional (2D) polyacrylamide gel electrophoresis (Fig. 8). In atrial cell membrane extracts 753 distinct membrane proteins were initially identified, and up to 104 proteins appeared to exhibit altered expression levels in cells from *Clcn3*$^{-/-}$ mice, compared to atrial cells from *Clcn3*$^{+/+}$ mice. To more reliably quantify actual changes in protein expression and minimize spurious results that might arise due to expected small variations in protein spot densities that normally occur from gel to gel, we established a minimal detection criterion of a twofold change in spot density. Using this criterion, comparisons of 2D gels from membrane extracts isolated from *Clcn3*$^{+/+}$ and*Clcn3*$^{-/-}$ mice (Fig. 8) consistently revealed significant changes in the expression of at least 35 distinct membrane proteins (6 missing proteins, 2 new proteins, 9 upregulated proteins, 15 downregulated proteins, and 2 translocated proteins) from hearts of *Clcn3*$^{-/-}$ mice compared to *Clcn3*$^{+/+}$ mice. One of the six missing proteins was identified as ClC-3 by Western blot analysis of the 2D gels. The location (molecular mass = 85 kDa and pI 6.9) of the ClC-3 protein spot (No. 3812) in the 2D gels from *Clcn3*$^{+/+}$ mice (□ in Fig. 8) is consistent with the predicted molecular mass of 84 kDa (10) and pI of 6.91 for ClC-3. Obviously, the compensatory changes in the animals in response to the targeted genetic manipulation are very complicated and the observed physiological or pathophysiological phenotypes of the *Clcn3*$^{-/-}$ mice cannot simply be attributed to changes in a single ClC-3 protein.

Alternatively, tissue-specific conditional or inducible knockout or knockin animal models may be more valuable in the phenotypic studies of specific Cl^- channels by limiting the effect of compensation on the phenotype. Therefore, we have generated the conditional heart-specific ClC-3 knockout (Fig. 9) (170) and knockin mice (169) and inducible heart-specific ClC-3 knockout mice (168). Figure 9 shows the results of echocardiographic evaluation of heart function and histological analysis of the conditional heart-specific ClC-3 knockout (*hsClcn3*$^{-/-}$) mouse heart. Echocardiography revealed marked signs of myocardial hypertrophy (a significant increase in left ventricular mass) and heart failure [a significant increase in LVIDs and reduction in interventricular septumthicknessat (IVSs), left ventricular ejection fraction (LVEF), and fractional shortening (%FS)] in the knockout mice compared to age-matched control mice (Fig. 9B). In addition, both left and right atria were significantly enlarged (Fig. 9C). These data strongly suggest that ClC-3 may play an important role in maintaining normal structure and function of the mammalian heart.

The cardiac-specific inducible ClC-3 knockout mice were maintained on a doxycycline diet to preserve ClC-3 expression; removal of doxycycline activates Cre recombinase to inactivate the *Clcn3* gene. Echocardiography revealed dramatically reduced LVEF and %FS, and severe signs of myocardial hypertrophy and heart failure in the knockout mice at both 1.5 and 3 weeks off doxycycline. In mice off doxycycline, time-dependent inactivation of ClC-3 gene expression was confirmed in atrial and ventricular cells by quantitative real time polymerase chain reaction (qRT-PCR) and Western blot analysis. Electrophysiological examination of native $I_{Cl,vol}$ in isolated atrial and ventricular myocytes 3 weeks off doxycycline revealed a complete elimination of the currents, whereas at 1.5 weeks, $I_{Cl,vol}$ current densities were significantly reduced, compared to age-matched control mice maintained on doxycycline (Fig. 10). These results indicate that ClC-3 is a key component of native $I_{Cl,vol}$ in mammalian heart and plays a significant cardioprotective role in

maintenance of normal heart structure and also in the protection of the heart against cardiac hypertrophy and failure under pathophysiological conditions.

In the transgenic mice with cardiac-specific overexpression of the human short ClC-3 isoform (sClC-3), Northern and Western blot analyses demonstrated that mRNA and protein levels of the short isoform (sClC-3) in the heart were significantly increased in hsClC-3-overexpressing (OE) mice compared with WT mice (169). Heart weight/bodyweight ratios for OE mice were significantly smaller compared with age-matched WT mice. Electrocardiogram recordings indicated no difference at rest, whereas echocardiographic recordings revealed consistent reductions in left ventricular diastolic diameter, left ventricular posterior wall thickness at end of diastole and interventricular septum thickness in diastole in OE mice (Fig. 10). The $I_{Cl,vol}$ current densities in atrial cardiomyocytes were significantly increased by ClC-3 overexpression compared with WT cells. No differences in properties of $I_{Cl,vol}$ in OE and WT atrial myocytes were observed in terms of outward rectification, anion permeability [I(−) > Cl(−) > Asp(−)] and inhibition by 4,4′-diisothiocyanatostilbene-2,2′-disulphonic acid and glibenclamide. The $I_{Cl,vol}$ in atrial myocytes from both groups were totally abolished by phorbol-12,13-dibutyrate (a PKC activator) and by intracellular dialysis of an N-terminal anti-ClC-3 antibody. Cardiac cell volume measurements revealed a significant acceleration of the rate of RVD in OE myocytes compared with WT. The enhanced $I_{Cl,vol}$ and acceleration of the time course of RVD in atrial myocytes of OE mice is strong evidence supporting an essential role of sClC-3 in native $I_{Cl,vol}$ function in mouse atrial myocytes (169).

Phenotypic study of cardiac ClC-2 channels

Properties of ClC-2 encoded $I_{Cl,ir}$ in cardiac myocytes—ClC-2 was cloned originally from rat heart and brain (147). Later several alternatively spliced forms were cloned from several other tissues and species, including human (26–28,67–69,113,114). Expression of ClC-2 cDNA in *Xenopus* oocytes or mammalian cells resulted in Cl^- currents which are activated by hyperpolarization, cell swelling, and acidosis and have an inwardly rectifying *I-V* relationship (26–28,68,69,95,128).

The endogenous $I_{Cl,ir}$ with biophysical and pharmacological properties similar to the Cl^- currents generated by expression of *ClC-2* gene was identified in native cardiac myocytes of guinea pig and mouse hearts for the first time in 2000 (56). Under conditions in which cationic inward rectifier channels were blocked, $I_{Cl,ir}$ was activated by membrane hyperpolarization (−40 to −140 mV). Under isotonic conditions, the current activated slowly with a biexponential time course (time constants averaging τ_1 = 179.76 ± 3.4 and τ_2 = 2073.66 ± 87.6 ms at −120 mV). Hypotonic cell swelling accelerated the activation (τ_1 = 97.5 ± 8.5 ms and τ_2 = 656.4 ± 113.6 ms at −120 mV) and increased the current amplitude whereas hypertonic cell shrinkage inhibited the current (Fig. 11). The inwardly rectifying current was carried by Cl^- and had an anion permeability sequence of $Cl^- > I^- \gg$ aspartate. $I_{Cl,ir}$ was blocked by 9-anthracene-carboxylic acid and cadmium but not by stilbene disulfonates and tamoxifen (56). Subsequently, similar $I_{Cl,ir}$ was found in rat atrial and subepicardial and subendocardial ventricular myocytes (100, 101). Acidosis (extracellular pH decreased from 7.4 to 6.5) increased $I_{Cl,ir}$, which may underlie the acidosis-induced depolarization of the resting membrane potential (100, 101). RT-PCR and Northern blot analysis confirmed transcriptional expression of ClC-2 in both atrial and ventricular tissues and isolated myocytes from mouse and guinea pig hearts (56). The expression of ClC-2 in the heart was further characterized by immunohistochemistry and Western blot analysis from several species (14). Later studies provided compelling evidence that $I_{Cl,ir}$ is encoded by ClC-2 and its alternatively spliced isoforms in the heart (16,89).

Because of its strong inward-rectification activation of the ClC-2 channels during the cardiac action potential will conduct mainly an inward current as a result of Cl^- efflux at negative membrane potentials and cause a depolarization of the resting membrane potential of cardiac cells. At membrane potentials more positive than the E_{Cl}, ClC-2 may conduct a small outward current as a result of Cl^- influx and may accelerate repolarization of the action potential. $I_{Cl,ir}$ under basal or isotonic conditions is small, but can be further activated by hypotonic cell swelling (56) and acidosis (100, 101). The volume sensitivity of the channel also suggests its role in cell volume regulation. The sensitivity of ClC-2 to $[H^+]_o$ and cell volume may be of pathological importance during hypoxia- or ischemia-induced acidosis or cell swelling. Therefore, it may be possible that the significance of $I_{Cl,ir}$ in the heart becomes more prominent under some pathological conditions (ischemia or hypoxia). As a matter of fact, ischemia and acidosis have consistently been shown to depolarize the resting membrane potential of cardiac myocytes, increase automaticity and cause lethal arrhythmias, although the mechanism has remained obscure (22, 85). It is reasonable to suggest that an increase in ClC-2 conductance could be responsible for these phenomena and be proarrhythmic. Drugs targeting ClC-2 channels could be antiarrhythmic. Therefore, the ClC-2 channels could have important clinical significance for such cardiac diseases as arrhythmias, ischemia, and reperfusion, and congestive heart failure. Activation of ClC-2 current should mainly cause a depolarization of the resting membrane potential and it is suggested that the acidosis-induced increase in $I_{Cl,ir}$ might underlie the depolarization of the resting membrane potential during acidosis or hypoxia (100,101).

Functional role of ClC-2 in pacemaker activity—It is possible that, in a manner analogous to the role and tissue distribution pattern of the cationic pacemaker channels (I_f) (44,45), the hyperpolarization-activated $I_{Cl,ir}$ through ClC-2 channels may normally play a much more prominent role in the S-A or atrial-ventricular nodal regions of the heart.

Our recent study found that $I_{Cl,ir}$ was indeed functionally expressed in guinea-pig sinoatrial nodal (SAN) cells (89). $I_{Cl,ir}$ in guinea-pig SAN cells activated upon cell membrane hyperpolarization and hypotonic challenge, has a strong inward rectification under symmetrical Cl^- conditions with a reversal potential close to the predicted value of E_{Cl}, and is inhibited by Cd^{2+} (Fig. 12). All these properties are identical to those of $I_{Cl,ir}$ in atrial and ventricular myocytes of several species, including guinea-pig, rat (16,56,100,101), and mouse (56). $I_{Cl,ir}$ is neither a part of the I_f nor a result of Cl^- regulation of the I_f activity (64) in SAN cells because (i) $I_{Cl,ir}$ can be recorded in the presence of a strong I_f blocker (20 mmol/L Cs^+) and in the absence of permeable cations; (ii) the reversal potential of $I_{Cl,ir}$ is close to the predicted E_{Cl}, suggesting the inward current is carried by Cl^-, not by cations; (iii) $I_{Cl,ir}$ but not I_f can be inhibited by Cd^{2+}; and (iv) $I_{Cl,ir}$ but not I_f is specifically inhibited by anti-*ClC-2* Ab.

Our data from RT-PCR and immunohistochemistry provided direct evidence for the expression of *ClC-2* in SAN cells (Fig. 13). In addition, dialysis of anti-*ClC-2* Ab but not the inactivated pre-absorbed Ab caused an inhibition of $I_{Cl,ir}$ but not I_f, $I_{Ca,L}$, I_{Ks}, and $I_{Cl,vol}$. These results further support that *ClC-2* is the gene responsible for the endogenous Cl,ir channels not only in atrial and ventricular myocytes (14, 16) but also in the SAN cells and that the Cl,ir in SAN cells may contribute to the regulation of pacemaker activity of the heart. Interestingly, the prevalence of functional endogenous $I_{Cl,ir}$ in the SAN cells (28/35, 80%) is apparently higher than that in the atrial or ventricular myocytes (56). Whether this difference is due to the higher molecular expression or the different activation mechanisms is a legitimate question which may be very difficult to get a clear answer. The first glance at the immunohistochemistry data shown in Figure 13 reveals no significant difference between the SAN and atrial tissues. Theoretically, a Western blot analysis of membrane fractions would help to quantitatively analyze the differences in the protein expression of

ClC-2 in the SAN cells and the atrial myocytes. But, practically, to carry out the Western blot analysis on the isolated membrane fractions from SAN cells it would need to collect enough SAN cells from the guinea-pig heart, which means not only a requirement for a pool of tens of hearts but also an isolation and selection of true SAN cells without contamination from the adjacent atrial cells. This is an extremely difficult task to accomplish. Although the confocal images of the SAN cells and atrail or ventricular myocytes would provide information on the subcellular distribution of ClC-2 channels in these cells it would not be able to give quantitative information for a decisive conclusion on the dynamic distribution of the ClC-2 channel protein and the relationship between the distribution and the function of the channels.

Because the E_{Cl} in cardiac cells under physiological conditions ranges between −65 and close −35 mV (5, 152), which is very to the maximum diastolic potential (MDP) of SAN cells, the contribution of $I_{Cl,ir}$ to SAN cell action potential is unique and also more complicated than the activation of I_f and other cation currents (Fig. 12). When the membrane potential is negative to E_{Cl}, opening of Cl,ir channel may conduct an inward current (Cl^- efflux), which will depolarize the MDP and increase the diastolic depolarization slope (DDs). At the beginning of DD, the impedance of the cell is very large and activation of a small current may contribute significantly to the depolarization of the action potential (178). Therefore, both the smaller instantaneous $I_{Cl,ir}$ activated at membrane potentials near the MDP and the larger time-dependent $I_{Cl,ir}$ activated at membrane potentials more negative than the MDP may contribute pacemaker current to the phase 4 depolarization of the action potential of SAN cells. When the membrane potential is positive to E_{Cl}, opening of Cl,ir channel may conduct an outward current (Cl^- influx) and make the membrane potential (possibly including the MDP) more negative. But the inward rectification property of Cl,ir may limit the amplitude of the outward current and its contribution to repolarization and APD. Since the MDP may be determined normally by multiple mechanisms (46, 110) such as I_f, I_{sus}, $I_{Ca.T}$, $I_{Ca,L}$, I_{NCX}, and possibly $I_{Cl,Ca}$ (157), and $I_{Cl,swell}$ (78), the contribution of changes in $I_{Cl,ir}$ to the MDP during hypotonic stress may be further complicated by changes in other ionic currents which may also responded to hypotonic cell swelling such as $I_{Cl,swell}$ (48, 60, 78) and I_{Ks} (130). In addition, activation of $I_{Cl,ir}$ may also cause a dynamic change in the E_{Cl} (145). The analysis of the relationship of the activation of $I_{Cl,ir}$ to the E_{Cl} and the consequent role of this relationship in determining the MDP has been limited by the lack of potent and specific $I_{Cl,ir}$ blocker. The identification of *ClC-2* as the gene responsible for Cl,ir channels in the heart and the availability of specific anti-*ClC-2* Ab provided us specific approach to effectively examine the functional role of Cl,ir in the heart.

In the isolated SAN cells, dialysis of anti-*ClC-2* Ab through the pipette solution for 20 min inhibited $I_{Cl,ir}$ (Fig. 14B) and reversed the hypotonic stress-induced increase in DDs and decrease in MDP, APA, APD_{90}, and CL under hypotonic conditions, suggesting that $I_{Cl,ir}$ may play a role in the regulation of DD and the firing rate of spontaneous action potential of SAN cells under stressed conditions. Anti-*ClC-2* Ab, however, did not have significant effect on the hypotonicity-induced shortening of APD_{50} (89). This may suggest that the contribution of the $I_{Cl,ir}$ to the repolarization at positive potentials is rather small because of its inward rectification property. These data may provide new mechanistic insight into the tonicity regulation of spontaneous beating rate in guinea-pig SAN reported by Ohba in 1986 (125). In that study, it was found that decreasing the osmolarity by 30% increased the heart rate by 6% and increasing the osmolarity to 130%, 150%, and 170% decreased the heart rate to 94%, 89%, and 73%, respectively (125).

As mentioned above, it is possible that the observed anti-*ClC-2* Ab-induced reduction in pacemaker activity under hypotonic conditions may be due to a nonspecific block of hypotonic activation of I_{Ks} (130) and $I_{Cl,swell}$ (48, 60, 78). But we found that anti-*ClC-2* Ab

failed to affect I_{Ks} and $I_{Cl,swell}$ under either isotonic or hypotonic conditions. These results are consistent with the observation that anti-*ClC-2* Ab has no effect on APD_{50} and strongly suggest that the activation of ClC-2 channels may play an important role in the DD and firing rate of SAN pacemaker activity but have very little impact on the repolarization at positive potentials during hypotonic stress. In addition, dialysis of preabsorbed anti-ClC-2 Ab did not cause any changes in the response of the SAN pacemaker activity to hypotonic stress (Fig. 15A and B) or in the hypotonic activation of $I_{Cl,ir}$. Therefore, it is highly unlikely that the anti-*ClC-2* Ab-induced reduction in the current amplitude of $I_{Cl,ir}$ and pacemaker activity in the SAN cells under hypotonic conditions are not due to the effects of anti-*ClC-2* Ab but the potential effects of dialysis with pipette solutions *per se*.

In agreement with our findings in the isolated cells, targeted inactivation of ClC-2 channels caused a decrease in HR, especially under exercise stress (Fig. 16). The resting HR of the $Clcn2^{-/-}$ mice was slower but not significantly different from the $Clcn2^{+/+}$ and $Clcn2^{+/-}$ mice. This may be explained by the fact that $I_{Cl,ir}$ through ClC-2 channels under basal or isotonic conditions is relatively small. It has been known that, however, $I_{Cl,ir}$ is activated in a larger scale by cell swelling (16,56), acidosis (100,101), and PKA phosphorylation (36, 37, 88, 96, 97). Indeed, hypoxia, ischemia, and acidosis have consistently been shown to increase automaticity and cause lethal arrhythmias, although the mechanism has remained obscure (22,48,60). Activation of $I_{Cl,ir}$ may explain, at least in part, the increase in automaticity under these stressed or pathological conditions (100, 101). We found that during acute exercise the maximal HR is lower in $Clcn2^{-/-}$ mice than in $Clcn2^{+/+}$ and $Clcn2^{+/-}$ mice, suggesting that activation of ClC-2 channels in the heart may contribute to the chronotropic response of the mouse to exercise stress. It is possible that activation of ClC-2 channels by β-stimulation induced PKA phosphorylation (36,37,66,88,96,98,139) may contribute to the regulation of HR during exercise. It has been known that several consensus PKA phosphorylation sites are well conserved in the ClC-2 sequences from different species (37). These results provide strong evidence for the molecular and functional expression of ClC-2 encoded endogenous Cl,ir channels in the SAN cells. The significance of $I_{Cl,ir}$ in the heart may become more prominent under stressed or pathological conditions. Our results may also shed new light on understanding mechanisms for arrhythmias such as sinus node dysfunction or sick sinus syndrome (46). Cardiac ClC-2 channels may thus represent new therapeutic targets for arrhythmias, congestive heart failure, and ischemic heart diseases.

Phenotypic study of Ca^{2+}-activated Cl^- channels in heart

Ca^{2+}-activated chloride channels (CACCs) are widely distributed in cardiac tissues and play important roles in the regulation of cardiac excitability. However, the molecular identity of this channel in the heart remains to be determined. CLCA-1 and bestrophins (79) were initially proposed as candidates for CACCs in cardiac tissues (123). It has been demonstrated that at least three members of the murine Bestrophin family, mBest1, mBest2 and mBest3, are expressed in mouse heart. Whole-cell patch clamp experiments with HEK cells transfected with cardiac mBest1 and mBest3 both elicited a calcium sensitive, time independent Cl^- current, suggesting mBest1 and mBest3 may function as pore-forming Cl^- channels that are activated by physiological levels of calcium (123, 124). Very recently, independent studies from three laboratories have identified a new gene, *TMEM16* (or *Ano1*), as a candidate for CACCs (21, 138, 175). The hTMEM16A mRNA is present in multiple human tissues, including heart, lung, placenta, liver, skeletal muscle, and small intestine (87). Whether TMEM16 forms the functional endogenous CACCs and how TMEME16 interacts with and the bestrophins in native cardiac myocytes remain to be explored.

CACCs and cardiac electrophysiology and arrhythmogenesis—Even though $I_{Cl,Ca}$ is also expected to be outwardly rectifying under physiological conditions the activation of $I_{Cl,Ca}$ will have considerably different effects on cardiac action potentials and resting membrane potential from those of CFTR and ClC-3 channels (Fig. 2). This is because the kinetic behavior of $I_{Cl,Ca}$ is significantly determined by the time course of the $[Ca^{2+}]_i$ transient (180). Normally, $I_{Cl,Ca}$ will have insignificant effects on the diastolic membrane potential, as resting $[Ca^{2+}]_i$ is low. When $[Ca^{2+}]_i$ is substantially increased above the physiological resting level, however, $I_{Cl,Ca}$ carries a significant amount of 4-AP-insensitive transient outward current sometimes included in current empirically identified as I_{to} (73). $I_{Cl,Ca}$ will activate early during the action potential in response to an increase in $[Ca^{2+}]_i$ associated with Ca^{2+}-induced Ca^{2+} release, The time course of decline of the $[Ca^{2+}]_i$ transient will determine the extent to which $I_{Cl,Ca}$ contributes to early repolarization during phase 1. In the rabbit heart, it was found that 4-AP-insensitive I_{to} is larger in atria than in ventricles (73, 181). And in the left ventricles $I_{Cl,Ca}$ contributes to APD shortening in subendocardial myocytes but not in subepicardial myocytes. These differences in functional expression of $I_{Cl,Ca}$ may reduce the electrical heterogeneity in the left ventricle (153). In Ca^{2+}-overloaded cardiac preparations, $I_{Cl,Ca}$ can contribute to the arrhythmogenic transient inward current (I_{TI}, see Fig. 17) (179). I_{TI} produces delayed afterdepolarization (DAD) (93) and induces triggered activity, which is an important mechanism for abnormal impulse formation. In sheep Purkinje and ventricular myocytes, activation of $I_{Cl,Ca}$ was found to induce DAD and plateau transient repolarization (155). Therefore, blockade of $I_{Cl,Ca}$ may be potentially antiarrhythmogenic by reducing DAD amplitude and triggered activity based on DAD. However, the role of $I_{Cl,Ca}$ in phase 1 repolarization and the generation of EAD and DAD of either normal or failing human heart seem very limited (156). Therefore, the clinical relevance of $I_{Cl,Ca}$ blockers remain to be determined.

$I_{Cl,Ca}$ in myocardial hypertrophy and heart failure—The critical role of Ca^{2+} in cardiac development, function, and disease is undisputable. Despite the heterogeneous etiology and overt manifestations of heart failure, abnormalities in Ca^{2+} handling are prominent, and alterations in Ca^{2+} homeostasis are a hallmark of myocardial hypertrophy and heart failure (86). Ca^{2+} transients in failing cardiac myocytes, for example, are characterized by diminished amplitude, elevated diastolic Ca^{2+} levels, and prolonged decay of the Ca^{2+} transients. In noncardiac cells, $I_{Cl,Ca}$ could be an important mediator of apoptosis (62). But, information on the possible involvement of $I_{Cl,Ca}$ in heart failure is currently very limited. It is reported that $I_{Cl,Ca}$ may play little, if any, role in the electrical remodeling of human end-stage failing heart (154, 156).

Phenomics and Its Application in the Study of Cardiac Chloride Channels

The remarkable similarity of mouse and human genomes, in both synteny and sequence, unconditionally validates the mouse as an exceptional model organism for understanding human biology. As described above, functional genomics through the examination and characterization of the phenotypic changes associated with loss of function or gain of function through targeted gene knockout or knockin in the mouse provides the direct and effective approach to the investigation of Cl^- channel gene function in the heart. However, major problems in the attempt to unravel the divergence of genotypic and phenotypic patterns of the genetically engineered mice and their disease models still await solutions. Although global knockout mice are invaluable experimental models and provide an excellent entry point for understanding complex function of mammalian genes, the compensatory changes in the animals in response to the targeted genetic manipulation as beneficial effects for the animal's survival (75, 174) may introduce complications in understanding the phenotypes of the animals. Even though the loss of the product of the targeted gene can be verified, the upregulation of other genes in the vicinity of the targeting

can occur (118) and may readily escape detection. Such upregulation could have an important effect on the observed phenotype. A knockout may not always be a knockout such as when the targeted gene is widely or ubiquitously expressed, when alternative splicing variants of the gene exist (94), and when functional channels are actually heteromultimeric and the structure might be associated with modulatory subunits (63). Accessory proteins may be involved in the determination of the stability of the channel complex in the membrane and in the modulation of biophysical, pharmacological, and regulatory properties of the channel. A Cl^- channel may function as a multiprotein complex or functional module, which may be composed of a pore forming subunit for ion transportation, auxiliary subunits for modulating pore gating, and proteins as second messengers tightly coupled to channel function (Fig. 4) (162). These proteins might be intimately linked to certain physiological functions and belong to the same subproteome. Manipulation of one gene in the subproteome may cause changes in other proteins of the same subproteome. Therefore, the functional consequences of disrupting the specific gene are very difficult to predict unless the changes in the entire subproteome are examined. Therefore, caution should be taken when conventional global gene knockout animals are used in phenotypic studies. Alternatively, tissue-specific conditional or inducible knockout or knockin animal models may be more valuable in the phenotypic studies of specific Cl^- channels by limiting the effect of compensation on the phenotype. On the other hand, previous studies of cardiovascular traits using different strains of inbred mice found that cardiovascular phenotypes are unlikely to segregate according to global phylogeny, but rather be governed by smaller, local differences in the genetic architecture of the various strains (6). It has also been commonly demonstrated that similar phenotypes can be attained from alternative protein pathways involving different gene products and many phenotypic changes may actually be a result of posttranslational modifications such as protein phosphorylation or dephosphorylation. Therefore, it is clear that conventional functional genomics may provide only limited information on the functional module of multiprotein complexes. We are now facing the challenge of a major paradigm shift to develop systematic approaches to the study of integrated Cl^- channel functions (48). Further investigations of the cellular and molecular mechanisms by which the cardiac Cl^- channel proteins function to impart physiological or pathophysiological phenotypes require a phenomic approach that would allow the transition from focused genotype/phenotype studies to a global genome/proteome/phenome-wide characterization of cardiac Cl^- channels in the heart in the context of health and disease.

Phenome and phenomics

Just as the genome and proteome signify all of an organism's genes and proteins, a phenome is the sum total of all phenotypes, including phenotypic traits due to either environmental influences or genetic variation such as single nucleotide polymorphisms, or a combination of the two, expressed by an organism or species. Similar to forward genetic approach where a particular trait or phenotype is the start to the discovery of the causal gene, phenomics is a forward genomic approach where the high-dimensional phenotypic data on an organism-wide scale is used to systemically delineate the nature of phenotypes and how they are determined, particularly in relation to the set of all genes (genome) or all proteins (proteome) (7).

Although it seems that phenome and phenomics are defined in analogy to genome and genomics, respectively, the concept of phenome and phenomics can actually be rooted way back to the pregenome era. As early as the mid-1960s phenetics, which involves the establishment of interobject similarities based on all available data from the objects, was used as a systematic approach to the classification of a set of organisms or objects by many investigators, most of them evolutionary biologists (7,38,102,119,143). The phenetic

approach had also been used by taxonomists in processing their material by intuitively grouping together individuals sharing a majority of characteristics in common.

In their description of the artificial worlds models of evolutionary systems in 1989, Conrad and Rizki (35) not only used the term of "phenome" but also described the embryo concept of "phenomics" for the very first time as follows:

> "The artificial world comprises an artificial environment, with mass components, energy input, and physical states. It also comprises artificial organisms, including a genome, a phenome, and a (developmental) map that connects the genome to the phenome. Mass components are cycled and space is limited. The evolution process results, as in nature, from genetic variation combined with natural selection imposed by the finiteness of the environment. The selection criteria (fitness values) are not imposed, but rather emerge from the interactions of the organisms with each other and with the environment. The dynamics at the population level also emerges from these basic interactions."

Later, especially in the postgenome era, many researchers have proposed that phenomics is the natural complement to genome sequencing as a crucial approach to a rapid advance in the understanding of human biology, physiology, pathophysiology, and diseases (8, 19, 72, 135–137). With the availability of the complete sequence of the mouse genome and the recognition of that mice are ideal for deciphering how the mammalian genome translates into the phenome as the mouse genome shares the high sequence homology with that of human genome the Jackson Laboratory initiated the Mouse Phenome Project in May 2000 to collect baseline phenotypic data on commonly used and genetically diverse inbred mouse strains and make this information publicly available through a web-accessible database (9, 127). The Mouse Phenome Database provides investigators with tools and detailed protocols for exploring both raw phenotypic data and comparative summary analyses, which enables investigators to identify appropriate strains for physiological testing, drug discovery, toxicology studies, mutagenesis, modeling human diseases, quantitative trait loci analyses and identification of new genes and unraveling the influence of environment on genotype (9, 127). By analogy with the Human Genome Project, Freimer and Sabatti proposed a Human Phenome Project (HPP) in 2003 as an organized international effort to conduct genome-wide genotyping on a massive scale. They proposed that the HPP would create phenomic databases with comprehensive assemblages of systematically collected phenotypic information and would develop new approaches for analyzing such phenotypic data (65). However, the advances in the phenomics studies have been stagnant with most investigators are still satisfied with conventional measurement of a limited and isolated set of phenotypes that seem the most relevant and important. Although it is now increasingly realized that phenotypes are the manifestation of the sum of network effects of multiple genes and proteins the transition from the Mendelian "one gene—one phenotype" rule to a "mutigene —multiphenotype" paradigm is still in its germinal phase of development.

Application of Phenomics in the study of cardiac chloride channels

Phenomics is a forward genetic approach where researchers start with a particular trait or phenotype and discover the causal gene. The application of phenomics approach in the study of cardiac Cl^- channels will focus on the systematic understanding of causal relationships between cardiovascular traits and Cl^- channel genes in the context of health and disease on a genome/proteome-wide scale. One of the powerful and direct methods for phenome analysis is to examine and characterize the phenomic changes associated with genomic/proteomic changes caused by specific "loss-of-function" or "gain-of-function" gene mutations in the mouse. The examination of any specific phenotype of these mice involves considering the complex genetic contributions to that outward manifestation from the entire genome and

proteome. Practically, therefore, phenomics studies of cardiac Cl^- channels require broad scientific expertise in genetics, molecular biology, cell biology, systems biology, statistics, mathematical modeling, bioinformatics, computer sciences, and phenotypic expression and analysis, and these experts of different disciplines must be capable of communicating effectively and collaboratively designing and executing translational research projects on a large scale. With the rapid increase of available high-throughput phenotyping technologies and conceptual, analytical, and bioinformatics approaches the time is now ripe for the phenomic study of cardiac Cl^- channels.

Conclusion

Recent efforts have provided strong evidence that Cl^- channels may play an important role in cardiac diseases, including arrhythmias, myocardial ischemia, hypertrophy, and heart failure. Although genetically engineered mice are invaluable experimental models and functional genomics remains a powerful approach to understanding the function of cardiac Cl^- channels, the complete understanding of the cellular and molecular mechanisms by which the cardiac Cl^- channel proteins function to impart physiological or pathophysiological phenotypes may require a phenomic approach to characterize the phenotypes of cardiac Cl^- channels on a genome- and proteome-wide scale in the context of health and disease.

Acknowledgments

The research in the Laboratory of Cardiovascular Phenomics, Center of Biomedical Research Excellence and the Department of Pharmacology, University of Nevada, School of Medicine is supported by grants from the National Institutes of Health (HL63914, HL106256, and HL113598), National Center of Research Resources (NCRR, P20RR15581), American Heart Association Western States Affiliate Grant-in-Aid (#11GRNT7610161), and American Diabetes Association Innovation Award (#07-8-IN-08).

References

1. Bahinski A, Nairn AC, Greengard P, Gadsby DC. Chloride conductance regulated by cyclic AMP-dependent protein kinase in cardiac myocytes. Nature. 1989; 340:718–721. [PubMed: 2475783]
2. Baker MA, Lane DJ, Ly JD, De Pinto V, Lawen A. VDAC1 is a transplasma membrane NADH-ferricyanide reductase. J Biol Chem. 2004; 279:4811–4819. [PubMed: 14573604]
3. Batthish M, Diaz RJ, Zeng HP, Backx PH, Wilson GJ. Pharmacological preconditioning in rabbit myocardium is blocked by chloride channel inhibition. Cardiovasc Res. 2002; 55:660–671. [PubMed: 12160963]
4. Baumgarten CM, Clemo HF. Swelling-activated chloride channels in cardiac physiology and pathophysiology. Prog Biophys Mol Biol. 2003; 82:25–42. [PubMed: 12732266]
5. Baumgarten CM, Fozzard HA. Intracellular chloride activity in mammalian ventricular muscle. Am J Physiol. 1981; 241:C121–C129. [PubMed: 6974504]
6. Berthonneche C, Peter B, Schupfer F, Hayoz P, Kutalik Z, Abriel H, Pedrazzini T, Beckmann JS, Bergmann S, Maurer F. Cardiovascular response to beta-adrenergic blockade or activation in 23 inbred mouse strains. PLoS ONE. 2009; 4:e6610. [PubMed: 19672458]
7. Bilder RM, Sabb FW, Cannon TD, London ED, Jentsch JD, Parker DS, Poldrack RA, Evans C, Freimer NB. Phenomics: The systematic study of phenotypes on a genome-wide scale. Neuroscience. 2009; 164:30–42. [PubMed: 19344640]
8. Blume AJ, Beasley J, Goldstein NI. The use of peptides in Diogenesis: A novel approach to drug discovery and phenomics. Biopolymers. 2000; 55:347–356. [PubMed: 11169925]
9. Bogue MA, Grubb SC. The Mouse Phenome Project. Genetica. 2004; 122:71–74. [PubMed: 15619963]

10. Borsani G, Rugarli EI, Taglialatela M, Wong C, Ballabio A. Characterization of a human and murine gene (CLCN3) sharing similarities to voltage-gated chloride channels and to a yeast integral membrane protein. Genomics. 1995; 27:131–141. [PubMed: 7665160]
11. Boujaoude LC, Bradshaw-Wilder C, Mao C, Cohn J, Ogretmen B, Hannun YA, Obeid LM. Cystic fibrosis transmembrane regulator regulates uptake of sphingoid base phosphates and lysophosphatidic acid: Modulation of cellular activity of sphingosine 1-phosphate. J Biol Chem. 2001; 276:35258–35264. [PubMed: 11443135]
12. Bozeat N, Dwyer L, Ye L, Yao T, Duan D. The role of ClC-3 chloride channels in early and late ischemic preconditioning in mouse heart. FASEB J. 2005; 19(4):A694–A695.
13. Bozeat N, Dwyer L, Ye L, Yao TY, Hatton WJ, Duan D. *VSOACs* play an important cardioprotective role in late ischemic preconditioning in mouse heart. Circulation. 2006; 114(1425):272–273.
14. Britton FC, Hatton WJ, Rossow CF, Duan D, Hume JR, Horowitz B. Molecular distribution of volume-regulated chloride channels (ClC-2 and ClC-3) in cardiac tissues. Am J Physiol Heart Circ Physiol. 2000; 279:H2225–H2233. [PubMed: 11045957]
15. Britton FC, Ohya S, Horowitz B, Greenwood IA. Comparison of the properties of CLCA1 generated currents and I(Cl(Ca)) in murine portal vein smooth muscle cells. J Physiol. 2002; 539:107–117. [PubMed: 11850505]
16. Britton FC, Wang GL, Huang ZM, Ye L, Horowitz B, Hume JR, Duan D. Functional characterization of novel alternatively spliced ClC-2 chloride channel variants in the heart. J Biol Chem. 2005; 280:25871–25880. [PubMed: 15883157]
17. Browe DM, Baumgarten CM. Stretch of beta 1 integrin activates an outwardly rectifying chloride current via FAK and Src in rabbit ventricular myocytes. J Gen Physiol. 2003; 122:689–702. [PubMed: 14610020]
18. Browe DM, Baumgarten CM. Angiotensin II (AT1) receptors and NADPH oxidase regulate Cl- current elicited by beta1 integrin stretch in rabbit ventricular myocytes. J Gen Physiol. 2004; 124:273–287. [PubMed: 15337822]
19. Burd L, Klug MG, Martsolf JT, Kerbeshian J. Fetal alcohol syndrome: Neuropsychiatric phenomics. Neurotoxicol Teratol. 2003; 25:697–705. [PubMed: 14624969]
20. Caille JP, Ruiz-Ceretti E, Schanne OF. Intracellular chloride activity in rabbit papillary muscle: Effect of ouabain. Am J Physiol. 1981; 240:C183–C188. [PubMed: 7235001]
21. Caputo A, Caci E, Ferrera L, Pedemonte N, Barsanti C, Sondo E, Pfeffer U, Ravazzolo R, Zegarra-Moran O, Galietta LJ. TMEM16A, a membrane protein associated with calcium-dependent chloride channel activity. Science. 2008; 322:590–594. [PubMed: 18772398]
22. Carmeliet E. Cardiac ionic currents and acute ischemia: From channels to arrhythmias. Physiol Rev. 1999; 79:917–1017. [PubMed: 10390520]
23. Chen H, Liu LL, Ye LL, McGuckin C, Tamowski S, Scowen P, Tian H, Murray K, Hatton WJ, Duan D. Targeted inactivation of cystic fibrosis transmembrane conductance regulator chloride channel gene prevents ischemic preconditioning in isolated mouse heart. Circulation. 2004; 110:700–704. [PubMed: 15289377]
24. Chen Z, Chua CC, Ho YS, Hamdy RC, Chua BH. Overexpression of Bcl-2 attenuates apoptosis and protects against myocardial I/R injury in transgenic mice. Am J Physiol Heart Circ Physiol. 2001; 280:H2313–H2320. [PubMed: 11299236]
25. Choi BR, Hatton WJ, Hume JR, Liu T, Salama G. Low osmolarity transforms ventricular fibrillation from complex to highly organized, with a dominant high-frequency source. Heart Rhythm. 2006; 3:1210–1220. [PubMed: 17018354]
26. Cid LP, Montrose-Rafizadeh C, Smith DI, Guggino WB, Cutting GR. Cloning of a putative human voltage-gated chloride channel (CIC-2) cDNA widely expressed in human tissues. Hum Mol Genet. 1995; 4:407–413. [PubMed: 7795595]
27. Cid LP, Niemeyer MI, Ramirez A, Sepulveda FV. Splice variants of a ClC-2 chloride channel with differing functional characteristics. Am J Physiol Cell Physiol. 2000; 279:C1198–C1210. [PubMed: 11003600]
28. Cid LP, Ramirez A, Niemeyer MI, Sepulveda FV. Characterisation of ClC-2 chloride channel splice variants. J Physiol (Lond). 2000; 523P:4P.

29. Clemo HF, Baumgarten CM. Protein kinase C activation blocks ICl(swell) and causes myocyte swelling in a rabbit congestive heart failure model. Circulation. 1998; 98:I–695.
30. Clemo HF, Danetz JS, Baumgarten CM. Does ClC-3 modulate cardiac cell volume? Biophys J. 1999; 76:A203.
31. Clemo HF, Stambler BS, Baumgarten CM. Swelling-activated chloride current is persistently activated in ventricular myocytes from dogs with tachycardia-induced congestive heart failure. Circ Res. 1999; 84:157–165. [PubMed: 9933247]
32. Collardeau-Frachon S, Bouvier R, Le GC, Rivet C, Cabet F, Bellon G, Lachaux A, Scoazec JY. Unexpected diagnosis of cystic fibrosis at liver biopsy: A report of four pediatric cases. Virchows Arch. 2007; 451:57–64. [PubMed: 17554556]
33. Collier ML, Hume JR. Unitary chloride channels activated by protein kinase C in guinea pig ventricular myocytes. Circ Res. 1995; 76:317–324. [PubMed: 7530607]
34. Collier ML, Levesque PC, Kenyon JL, Hume JR. Unitary Cl- channels activated by cytoplasmic Ca2+ in canine ventricular myocytes. Circ Res. 1996; 78:936–944. [PubMed: 8620614]
35. Conrad M, Rizki MM. The artificial worlds approach to emergent evolution. Biosystems. 1989; 23:247–258. [PubMed: 2627568]
36. Cuppoletti J, Malinowska DH, Tewari KP, Li QJ, Sherry AM, Patchen ML, Ueno R. SPI-0211 activates T84 cell chloride transport and recombinant human ClC-2 chloride currents. Am J Physiol Cell Physiol. 2004; 287:C1173–C1183. [PubMed: 15213059]
37. Cuppoletti J, Tewari KP, Sherry AM, Ferrante CJ, Malinowska DH. Sites of protein kinase A activation of the human ClC-2 Cl(−) channel. J Biol Chem. 2004; 279:21849–21856. [PubMed: 15010473]
38. da Silva GA, Holt JG. Numerical taxonomy of certain coryneform bacteria. J Bacteriol. 1965; 90:921–927. [PubMed: 4954898]
39. Davies WL, Vandenberg JI, Sayeed RA, Trezise AE. Post-transcriptional regulation of the cystic fibrosis gene in cardiac development and hypertrophy. Biochem Biophys Res Commun. 2004; 319:410–418. [PubMed: 15178422]
40. De Mello WC. Heart failure: How important is cellular sequestration? The role of the renin-angiotensin-aldosterone system. J Mol Cell Cardiol. 2004; 37:431–438. [PubMed: 15276013]
41. Deng W, Baki L, Baumgarten CM. Endothelin signalling regulates volume-sensitive Cl- current via NADPH oxidase and mitochondrial reactive oxygen species. Cardiovasc Res. 2010; 88:93–100. [PubMed: 20444986]
42. Diaz RJ, Batthish M, Backx PH, Wilson GJ. Chloride channel inhibition does block the protection of ischemic preconditioning in myocardium. J Mol Cell Cardiol. 2001; 33:1887–1889. [PubMed: 11603930]
43. Diaz RJ, Losito VA, Mao GD, Ford MK, Backx PH, Wilson GJ. Chloride channel inhibition blocks the protection of ischemic preconditioning and hypo-osmotic stress in rabbit ventricular myocardium. Circ Res. 1999; 84:763–775. [PubMed: 10205144]
44. DiFrancesco D. Properties of the cardiac pacemaker (if) current. Boll Soc Ital Biol Sper. 1984; 60(Suppl 4):29–33. [PubMed: 6466486]
45. DiFrancesco D. Funny channels in the control of cardiac rhythm and mode of action of selective blockers. Pharmacol Res. 2006; 53:399–406. [PubMed: 16638640]
46. Dobrzynski H, Boyett MR, Anderson RH. New insights into pacemaker activity: Promoting understanding of sick sinus syndrome. Circulation. 2007; 115:1921–1932. [PubMed: 17420362]
47. Du XY, Sorota S. Cardiac swelling-induced chloride current depolarizes canine atrial myocytes. Am J Physiol. 1997; 272:H1904–H1916. [PubMed: 9139978]
48. Duan D. Phenomics of cardiac chloride channels: The systematic study of chloride channel function in the heart. J Physiol. 2009; 587:2163–2177. [PubMed: 19171656]
49. Duan D, Cowley S, Horowitz B, Hume JR. A serine residue in ClC-3 links phosphorylation-dephosphorylation to chloride channel regulation by cell volume. J Gen Physiol. 1999; 113:57–70. [PubMed: 9874688]
50. Duan D, Fermini B, Nattel S. Sustained outward current observed after I(to1) inactivation in rabbit atrial myocytes is a novel Cl- current. Am J Physiol. 1992; 263:H1967–H1971. [PubMed: 1481920]

51. Duan D, Fermini B, Nattel S. Alpha-adrenergic control of volume-regulated Cl- currents in rabbit atrial myocytes. Characterization of a novel ionic regulatory mechanism. Circ Res. 1995; 77:379–393. [PubMed: 7542183]
52. Duan D, Hume JR, Nattel S. Evidence that outwardly rectifying Cl- channels underlie volume-regulated Cl- currents in heart. Circ Res. 1997; 80:103–113. [PubMed: 8978329]
53. Duan D, Liu L, Wang GL, Ye L, Tian H, Yao Y, Chen A, Duan M, Hatton W. Cell volume-regulated ion channels and ionic remodeling in hypertrophied mouse heart. J Cardiac Failure. 2004; 10:S72.
54. Duan D, Nattel S. Properties of single outwardly rectifying Cl- channels in heart. Circ Res. 1994; 75:789–795. [PubMed: 7923623]
55. Duan D, Winter C, Cowley S, Hume JR, Horowitz B. Molecular identification of a volume-regulated chloride channel. Nature. 1997; 390:417–421. [PubMed: 9389484]
56. Duan D, Ye L, Britton F, Horowitz B, Hume JR. UltraRapid communications : A novel anionic inward rectifier in native cardiac myocytes. Circ Res. 2000; 86:485. [PubMed: 10700455]
57. Duan D, Ye L, Britton F, Miller LJ, Yamazaki J, Horowitz B, Hume JR. Purinoceptor-coupled Cl- channels in mouse heart: A novel, alternative pathway for CFTR regulation. J Physiol. 1999; 521(Pt 1):43–56. [PubMed: 10562333]
58. Duan D, Zhong J, Hermoso M, Satterwhite CM, Rossow CF, Hatton WJ, Yamboliev I, Horowitz B, Hume JR. Functional inhibition of native volume-sensitive outwardly rectifying anion channels in muscle cells and Xenopus oocytes by anti-ClC-3 antibody. J Physiol. 2001; 531:437–444. [PubMed: 11230516]
59. Duan DD. Volume matters: Novel roles of the volume-regulated CLC-3 channels in hypertension-induced cerebrovascular remodeling. Hypertension. 2010; 56:346–348. [PubMed: 20644007]
60. Duan DY, Liu LL, Bozeat N, Huang ZM, Xiang SY, Wang GL, Ye L, Hume JR. Functional role of anion channels in cardiac diseases. Acta Pharmacol Sin. 2005; 26:265–278. [PubMed: 15715921]
61. Dutzler R, Campbell EB, Cadene M, Chait BT, MacKinnon R. X-ray structure of a ClC chloride channel at 3.0 A reveals the molecular basis of anion selectivity. Nature. 2002; 415:287–294. [PubMed: 11796999]
62. Elble RC, Pauli BU. Tumor suppression by a proapoptotic calcium-activated chloride channel in mammary epithelium. J Biol Chem. 2001; 276:40510–40517. [PubMed: 11483609]
63. Estevez R, Boettger T, Stein V, Birkenhager R, Otto E, Hildebrandt F, Jentsch TJ. Barttin is a Cl- channel beta-subunit crucial for renal Cl- reabsorption and inner ear K +secretion. Nature. 2001; 414:558–561. [PubMed: 11734858]
64. Frace AM, Maruoka F, Noma A. Control of the hyperpolarization-activated cation current by external anions in rabbit sino-atrial node cells. J Physiol (Lond). 1992; 453:307–318. [PubMed: 1281504]
65. Freimer N, Sabatti C. The human phenome project. Nat Genet. 2003; 34:15–21. [PubMed: 12721547]
66. Fritsch J, Edelman A. Modulation of the hyperpolarization-activated Cl- current in human intestinal T84 epithelial cells by phosphorylation. J Physiol. 1996; 490(Pt 1):115–128. [PubMed: 8745282]
67. Furukawa T, Horikawa S, Terai T, Ogura T, Katayama Y, Hiraoka M. Molecular cloning and characterization of a novel truncated from (ClC-2 beta) of ClC-2 alpha (ClC-2G) in rabbit heart. FEBS Lett. 1995; 375:56–62. [PubMed: 7498481]
68. Furukawa T, Ogura T, Katayama Y, Hiraoka M. Characteristics of rabbit ClC-2 current expressed in Xenopus oocytes and its contribution to volume regulation. Am J Physiol. 1998; 274:C500–C512. [PubMed: 9486141]
69. Furukawa T, Ogura T, Zheng YJ, Tsuchiya H, Nakaya H, Katayama Y, Inagaki N. Phosphorylation and functional regulation of ClC-2 chloride channels expressed in Xenopus oocytes by M cyclin-dependent protein kinase. J Physiol. 2002; 540:883–893. [PubMed: 11986377]
70. Gadsby DC, Nairn AC. Control of CFTR channel gating by phosphorylation and nucleotide hydrolysis. Physiol Rev. 1999; 79:S77–S107. [PubMed: 9922377]

71. Gao L, Kim KJ, Yankaskas JR, Forman HJ. Abnormal glutathione transport in cystic fibrosis airway epithelia. Am J Physiol. 1999; 277:L113–L118. [PubMed: 10409237]
72. Gerlai R. Phenomics: Fiction or the future? Trends Neurosci. 2002; 25:506–509. [PubMed: 12220878]
73. Giles WR, Imaizumi Y. Comparison of potassium currents in rabbit atrial and ventricular cells. J Physiol. 1988; 405:123–145. [PubMed: 2855639]
74. Guan YY, Wang GL, Zhou JG. The ClC-3 Cl- channel in cell volume regulation, proliferation and apoptosis in vascular smooth muscle cells. Trends Pharmacol Sci. 2006; 27:290–296. [PubMed: 16697056]
75. Guggino SE. Can we generate new hypotheses about Dent disease from gene analysis? Exp Physiol. 2009; 94:191–196. [PubMed: 18931044]
76. Guggino WB, Banks-Schlegel SP. Macromolecular interactions and ion transport in cystic fibrosis. Am J Respir Crit Care Med. 2004; 170:815–820. [PubMed: 15447951]
77. Guggino WB, Stanton BA. New insights into cystic fibrosis: Molecular switches that regulate CFTR. Nat Rev Mol Cell Biol. 2006; 7:426–436. [PubMed: 16723978]
78. Hagiwara N, Masuda H, Shoda M, Irisawa H. Stretch-activated anion currents of rabbit cardiac myocytes. J Physiol (Lond). 1992; 456:285–302. [PubMed: 1284078]
79. Hartzell C, Putzier I, Arreola J. Calcium-activated chloride channels. Annu Rev Physiol. 2005; 67:719–758. [PubMed: 15709976]
80. Harvey RD. Cardiac chloride currents. News Physiol Sci. 1996; 11:175–181.
81. Harvey RD, Hume JR. Autonomic regulation of a chloride current in heart. Science. 1989; 244:983–985. [PubMed: 2543073]
82. Harvey RD, Hume JR. Histamine activates the chloride current in cardiac ventricular myocytes. J Cardiovas Electrophysiol. 1990; 1:309–317.
83. Hermoso M, Satterwhite CM, Andrade YN, Hidalgo J, Wilson SM, Horowitz B, Hume JR. ClC-3 is a fundamental molecular component of volume-sensitive outwardly rectifying Cl- channels and volume regulation in HeLa cells and Xenopus laevis oocytes. J Biol Chem. 2002; 277:40066–40074. [PubMed: 12183454]
84. Heusch G, Liu GS, Rose J, Cohen MV, Downey JM. No confirmation for a causal role of volume-regulated chloride channels in ischemic preconditioning in rabbits. J Mol Cell Cardiol. 2000; 32:2279–2285. [PubMed: 11113003]
85. Hiraoka M, Kawano S, Hirano Y, Furukawa T. Role of cardiac chloride currents in changes in action potential characteristics and arrhythmias. Cardiovasc Res. 1998; 40:23–33. [PubMed: 9876314]
86. Houser SR, Piacentino V III, Weisser J. Abnormalities of calcium cycling in the hypertrophied and failing heart. J Mol Cell Cardiol. 2000; 32:1595–1607. [PubMed: 10966823]
87. Huang X, Godfrey TE, Gooding WE, McCarty KS Jr, Gollin SM. Comprehensive genome and transcriptome analysis of the 11q13 amplicon in human oral cancer and synteny to the 7F5 amplicon in murine oral carcinoma. Genes Chromosomes Cancer. 2006; 45:1058–1069. [PubMed: 16906560]
88. Huang ZM, Britton FC, An C, Yuan C, Ye L, Hatton WJ, Duan D. Characterization of ClC-2 channel/PKA interaction in mouse heart. FASEB J. 2008; 22:721.5. [PubMed: 17971398]
89. Huang ZM, Prasad C, Britton FC, Ye LL, Hatton WJ, Duan D. Functional role of CLC-2 chloride inward rectifier channels in cardiac sinoatrial nodal pacemaker cells. J Mol Cell Cardiol. 2009; 47:121–132. [PubMed: 19376127]
90. Hume JR, Duan D, Collier ML, Yamazaki J, Horowitz B. Anion transport in heart. Physiol Rev. 2000; 80:31–81. [PubMed: 10617765]
91. Hume JR, Wang GX, Yamazaki J, Ng LC, Duan D. CLC-3 chloride channels in the pulmonary vasculature. Adv Exp Med Biol. 2010; 661:237–247. [PubMed: 20204734]
92. Intengan HD, Schiffrin EL. Vascular remodeling in hypertension: Roles of apoptosis, inflammation, and fibrosis. Hypertension. 2001; 38:581–587. [PubMed: 11566935]
93. January CT, Fozzard HA. Delayed afterdepolarizations in heart muscle: Mechanisms and relevance. Pharmacol Rev. 1988; 40:219–227. [PubMed: 3065793]

94. Jentsch TJ, Stein V, Weinreich F, Zdebik AA. Molecular structure and physiological function of chloride channels. Physiol Rev. 2002; 82:503–568. [PubMed: 11917096]

95. Jordt SE, Jentsch TJ. Molecular dissection of gating in the ClC-2 chloride channel. EMBO J. 1997; 16:1582–1592. [PubMed: 9130703]

96. Kajita H, Omori K, Matsuda H. The chloride channel ClC-2 contributes to the inwardly rectifying Cl- conductance in cultured porcine choroid plexus epithelial cells. J Physiol. 2000; 523(Pt 2): 313–324. [PubMed: 10699077]

97. Kajita H, Whitwell C, Brown PD. Properties of the inward-rectifying Cl- channel in rat choroid plexus: Regulation by intracellular messengers and inhibition by divalent cations. Pflugers Arch. 2000; 440:933–940. [PubMed: 11041561]

98. Kajita H, Whitwell C, Brown PD. Properties of the inward-rectifying Cl- channel in rat choroid plexus: Regulation by intracellular messengers and inhibition by divalent cations. Pflugers Arch. 2000; 440:933–940. [PubMed: 11041561]

99. Kogan I, Ramjeesingh M, Li C, Kidd JF, Wang Y, Leslie EM, Cole SP, Bear CE. CFTR directly mediates nucleotide-regulated glutathione flux. EMBO J. 2003; 22:1981–1989. [PubMed: 12727866]

100. Komukai K, Brette F, Orchard CH. Electrophysiological response of rat atrial myocytes to acidosis. Am J Physiol Heart Circ Physiol. 2002; 283:H715–H724. [PubMed: 12124220]

101. Komukai K, Brette F, Pascarel C, Orchard CH. Electrophysiological response of rat ventricular myocytes to acidosis. Am J Physiol Heart Circ Physiol. 2002; 283:H412–H422. [PubMed: 12063316]

102. Krieg RE, Lockhart WR. Classification of enterobacteria based on overall similarity. J Bacteriol. 1966; 92:1275–1280. [PubMed: 5924265]

103. Kunzelmann K, Schreiber R, Boucherot A. Mechanisms of the inhibition of epithelial Na(+) channels by CFTR and purinergic stimulation. Kidney Int. 2001; 60:455–461. [PubMed: 11473626]

104. Kunzelmann K, Schreiber R, Nitschke R, Mall M. Control of epithelial Na+ conductance by the cystic fibrosis transmembrane conductance regulator. Pflugers Arch. 2000; 440:193–201. [PubMed: 10898518]

105. Lang F, Busch GL, Ritter M, Volkl H, Waldegger S, Gulbins E, Haussinger D. Functional significance of cell volume regulatory mechanisms. Physiol Rev. 1998; 78:247–306. [PubMed: 9457175]

106. Lemonnier L, Shuba Y, Crepin A, Roudbaraki M, Slomianny C, Mauroy B, Nilius B, Prevarskaya N, Skryma R. Bcl-2-dependent modulation of swelling-activated Cl- current and ClC-3 expression in human prostate cancer epithelial cells. Cancer Res. 2004; 64:4841–4848. [PubMed: 15256454]

107. Levesque PC, Hume JR. ATPo but not cAMPi activates a chloride conductance in mouse ventricular myocytes. Cardiovasc Res. 1995; 29:336–343. [PubMed: 7540110]

108. Li Y, Trush MA. Diphenyleneiodonium, an NAD(P)H oxidase inhibitor, also potently inhibits mitochondrial reactive oxygen species production. Biochem Biophys Res Commun. 1998; 253:295–299. [PubMed: 9878531]

109. Linsdell P, Hanrahan JW. Glutathione permeability of CFTR. Am J Physiol. 1998; 275:C323–C326. [PubMed: 9688865]

110. Liu J, Noble PJ, Xiao G, Abdelrahman M, Dobrzynski H, Boyett MR, Lei M, Noble D. Role of pacemaking current in cardiac nodes: Insights from a comparative study of sinoatrial node and atrioventricular node. Prog Biophys Mol Biol. 2007; 96:294–304. [PubMed: 17905415]

111. Liu L, Ye L, McGuckin C, Hatton WJ, Duan D. Disruption of Clcn3 gene in mice facilitates heart failure during pressure overload. J Gen Physiol. 2003; 122:76.

112. Liu YJ, Wang XG, Tang YB, Chen JF, Lv XF, Zhou JG, Guan YY. Simvastatin ameliorates rat cerebrovascular remodeling during hypertension via inhibition of volume-regulated chloride channel. Hypertension. 2010 in press.

113. Loewen ME, MacDonald DW, Gaspar KJ, Forsyth GW. Isoformspecific exon skipping in a variant form of ClC-2. Biochim Biophys Acta. 2000; 1493:284–288. [PubMed: 10978540]

114. Malinowska DH, Kupert EY, Bahinski A, Sherry AM, Cuppoletti J. Cloning, functional expression, and characterization of a PKA-activated gastric Cl- channel. Am J Physiol. 1995; 268:C191–C200. [PubMed: 7840147]
115. Miller FJ Jr. Filali M, Huss GJ, Stanic B, Chamseddine A, Barna TJ, Lamb FS. Cytokine activation of nuclear factor kappa B in vascular smooth muscle cells requires signaling endosomes containing Nox1 and ClC-3. Circ Res. 2007; 101:663–671. [PubMed: 17673675]
116. Minagawa N, Nagata J, Shibao K, Masyuk AI, Gomes DA, Rodrigues MA, LeSage G, Akiba Y, Kaunitz JD, Ehrlich BE, LaRusso NF, Nathanson MH. Cyclic AMP regulates bicarbonate secretion in cholangiocytes through release of ATP into bile. Gastroenterology. 2007; 133:1592–1602. [PubMed: 17916355]
117. Mizoguchi K, Maeta H, Yamamoto A, Oe M, Kosaka H. Amelioration of myocardial global ischemia/reperfusion injury with volume-regulatory chloride channel inhibitors in vivo. Transplantation. 2002; 73:1185–1193. [PubMed: 11981408]
118. Moore RC, Lee IY, Silverman GL, Harrison PM, Strome R, Heinrich C, Karunaratne A, Pasternak SH, Chishti MA, Liang Y, Mastrangelo P, Wang K, Smit AF, Katamine S, Carlson GA, Cohen FE, Prusiner SB, Melton DW, Tremblay P, Hood LE, Westaway D. Ataxia in prion protein (PrP)-deficient mice is associated with upregulation of the novel PrP-like protein doppel. J Mol Biol. 1999; 292:797–817. [PubMed: 10525406]
119. Moss WW, Webster WA. Phenetics and numerical taxonomy applied to systematic nematology. J Nematol. 1970; 2:16–25. [PubMed: 19322269]
120. Nagel G, Hwang TC, Nastiuk KL, Nairn AC, Gadsby DC. The protein kinase A-regulated cardiac Cl- channel resembles the cystic fibrosis transmembrane conductance regulator. Nature. 1992; 360:81–84. [PubMed: 1279437]
121. Nakajima T, Sugimoto T, Kurachi Y. Effects of anions on the G protein-mediated activation of the muscarinic K+ channel in the cardiac atrial cell membrane. Intracellular chloride inhibition of the GTPase activity of GK. J Gen Physiol. 1992; 99:665–682. [PubMed: 1607851]
122. Naren AP, Kirk KL. CFTR chloride channels: binding partners and regulatory networks. News Physiol Sci. 2000; 15:57–61. [PubMed: 11390879]
123. O'Driscoll KE, Hatton WJ, Burkin HR, Leblanc N, Britton FC. Expression, localization and functional properties of Bestrophin 3 channel isolated from mouse heart. Am J Physiol Cell Physiol. 2008; 295:C1610–C1624. [PubMed: 18945938]
124. O'Driscoll KE, Leblanc N, Britton FC. Molecular and functional characterization of murine Bestrophin 1 cloned from Heart. FASEB J. 2008; 22 1201.25.
125. Ohba M. Effects of tonicity on the pacemaker activity of guinea-pig sino-atrial node. Jpn J Physiol. 1986; 36:1027–1038. [PubMed: 2435940]
126. Okada Y, Shimizu T, Maeno E, Tanabe S, Wang X, Takahashi N. Volume-sensitive chloride channels involved in apoptotic volume decrease and cell death. J Membr Biol. 2006; 209:21–29. [PubMed: 16685598]
127. Paigen K, Eppig JT. A mouse phenome project. Mamm Genome. 2000; 11:715–717. [PubMed: 10967127]
128. Park K, Begenisich T, Melvin JE. Protein kinase A activation phosphorylates the rat ClC-2 Cl-channel but does not change activity. J Membr Biol. 2001; 182:31–37. [PubMed: 11426297]
129. Patel DG, Higgins RS, Baumgarten CM. Swelling-activated cl current, ICl,swell, is chronically activated in diseased human atrial myocytes. Biophys J. 2003; 84:233.
130. Rees SA, Vandenberg JI, Wright AR, Yoshida A, Powell T. Cell swelling has differential effects on the rapid and slow components of delayed rectifier potassium current in guinea pig cardiac myocytes. J Gen Physiol. 1995; 106:1151–1170. [PubMed: 8786354]
131. Reisin IL, Prat AG, Abraham EH, Amara JF, Gregory RJ, Ausiello DA, Cantiello HF. The cystic fibrosis transmembrane conductance regulator is a dual ATP and chloride channel. J Biol Chem. 1994; 269:20584–20591. [PubMed: 7519611]
132. Ren Z, Raucci FJ Jr. Browe DM, Baumgarten CM. Regulation of swelling-activated Cl(−) current by angiotensin II signalling and NADPH oxidase in rabbit ventricle. Cardiovasc Res. 2008; 77:73–80. [PubMed: 18006461]

133. Ruiz PE, Ponce ZA, Schanne OF. Early action potential shortening in hypoxic hearts: Role of chloride current(s) mediated by catecholamine release. J Mol Cell Cardiol. 1996; 28:279–290. [PubMed: 8729060]
134. Sabirov RZ, Okada Y. ATP release via anion channels. Purinergic Signal. 2005; 1:311–328. [PubMed: 18404516]
135. Sachar DB. Genomics and phenomics in Crohn's disease. Gastroenterology. 2002; 122:1161–1162. [PubMed: 11910366]
136. Schilling CH, Edwards JS, Palsson BO. Toward metabolic phenomics: Analysis of genomic data using flux balances. Biotechnol Prog. 1999; 15:288–295. [PubMed: 10356245]
137. Schork NJ. Genetics of complex disease: Approaches, problems, and solutions. Am J Respir Crit Care Med. 1997; 156:S103–S109. [PubMed: 9351588]
138. Schroeder BC, Cheng T, Jan YN, Jan LY. Expression cloning of TMEM16A as a calcium-activated chloride channel subunit. Cell. 2008; 134:1019–1029. [PubMed: 18805094]
139. Sherry AM, Stroffekova K, Knapp LM, Kupert EY, Cuppoletti J, Malinowska DH. Characterization of the human pH- and PKA-activated ClC-2G(2 alpha) Cl− channel. Am J Physiol. 1997; 273:C384–C393. [PubMed: 9277336]
140. Skach WR. CFTR: New members join the fold. Cell. 2006; 127:673–675. [PubMed: 17110327]
141. Solbach TF, Paulus B, Weyand M, Eschenhagen T, Zolk O, Fromm MF. ATP-binding cassette transporters in human heart failure. Naunyn Schmiedebergs Arch Pharmacol. 2008; 377:231–243. [PubMed: 18392808]
142. Sorota S. Swelling-induced chloride-sensitive current in canine atrial cells revealed by whole-cell patch-clamp method. Circ Res. 1992; 70:679–687. [PubMed: 1551194]
143. Soule M, Baker B. Phenetics of natural populations. IV. The population asymmetry parameter in the butterfly Coenonympha tullia. Heredity. 1968; 23:611–614. [PubMed: 5253588]
144. Spitzer KW, Walker JL. Intracellular chloride activity in quiescent cat papillary muscle. Am J Physiol. 1980; 238:H487–H493. [PubMed: 7377319]
145. Staley K, Smith R, Schaack J, Wilcox C, Jentsch TJ. Alteration of GABAA receptor function following gene transfer of the CLC-2 chloride channel. Neuron. 1996; 17:543–551. [PubMed: 8816717]
146. Sugita M, Yue Y, Foskett JK. CFTR Cl− channel and CFTR-associated ATP channel: Distinct pores regulated by common gates. EMBO J. 1998; 17:898–908. [PubMed: 9463368]
147. Thiemann A, Grunder S, Pusch M, Jentsch TJ. A chloride channel widely expressed in epithelial and non-epithelial cells. Nature. 1992; 356:57–60. [PubMed: 1311421]
148. Tomaselli GF, Marban E. Electrophysiological remodeling in hypertrophy and heart failure. Cardiovasc Res. 1999; 42:270–283. [PubMed: 10533566]
149. van Borren MM, Verkerk AO, Vanharanta SK, Baartscheer A, Coronel R, Ravesloot JH. Reduced swelling-activated Cl(−) current densities in hypertrophied ventricular myocytes of rabbits with heart failure. Cardiovasc Res. 2002; 53:869–878. [PubMed: 11922897]
150. Vandenberg JI, Bett GC, Powell T. Contribution of a swelling-activated chloride current to changes in the cardiac action potential. Am J Physiol. 1997; 273:C541–C547. [PubMed: 9277351]
151. Vaughan-Jones RD. Non-passive chloride distribution in mammalian heart muscle: Micro-electrode measurement of the intracellular chloride activity. J Physiol (Lond). 1979; 295:83–109. [PubMed: 521996]
152. Vaughan-Jones RD. Chloride activity and its control in skeletal and cardiac muscle. Philos Trans R Soc Lond B Biol Sci. 1982; 299:537–548. [PubMed: 6130545]
153. Verkerk AO, Tan HL, Ravesloot JH. Ca2+-activated Cl− current reduces transmural electrical heterogeneity within the rabbit left ventricle. Acta Physiol Scand. 2004; 180:239–247. [PubMed: 14962005]
154. Verkerk AO, Veldkamp MW, Baartscheer A, Schumacher CA, Klopping C, van Ginneken AC, Ravesloot JH. Ionic mechanism of delayed afterdepolarizations in ventricular cells isolated from human end-stage failing hearts. Circulation. 2001; 104:2728–2733. [PubMed: 11723027]

155. Verkerk AO, Veldkamp MW, Bouman LN, van Ginneken AC. Calcium-activated Cl(−) current contributes to delayed afterdepolarizations in single Purkinje and ventricular myocytes. Circulation. 2000; 101:2639–2644. [PubMed: 10840017]
156. Verkerk AO, Wilders R, Coronel R, Ravesloot JH, Verheijck EE. Ionic remodeling of sinoatrial node cells by heart failure. Circulation. 2003; 108:760–766. [PubMed: 12885752]
157. Verkerk AO, Wilders R, Zegers JG, van Borren MM, Ravesloot JH, Verheijck EE. Ca(2+)-activated Cl(−) current in rabbit sinoatrial node cells. J Physiol. 2002; 540:105–117. [PubMed: 11927673]
158. Vilela RM, Lands LC, Meehan B, Kubow S. Inhibition of IL-8 release from CFTR-deficient lung epithelial cells following pre-treatment with fenretinide. Int Immunopharmacol. 2006; 6:1651–1664. [PubMed: 16979119]
159. Volk AP, Heise CK, Hougen JL, Artman CM, Volk KA, Wessels D, Soll DR, Nauseef WM, Lamb FS, Moreland JG. CLC-3 and ICLswell are required for normal neutrophil chemotaxis and shape change. J Biol Chem. 2008; 283:34315–34326. [PubMed: 18840613]
160. Walsh KB, Long KJ. Properties of a protein kinase C-activated chloride current in guinea pig ventricular myocytes. Circ Res. 1994; 74:121–129. [PubMed: 8261585]
161. Wang GX, Hatton WJ, Wang GL, Zhong J, Yamboliev I, Duan D, Hume JR. Functional effects of novel anti-ClC-3 antibodies on native volume-sensitive osmolyte and anion channels in cardiac and smooth muscle cells. Am J Physiol Heart Circ Physiol. 2003; 285:H1453–H1463. [PubMed: 12816749]
162. Wang X, Venable J, LaPointe P, Hutt DM, Koulov AV, Coppinger J, Gurkan C, Kellner W, Matteson J, Plutner H, Riordan JR, Kelly JW, Yates JR III, Balch WE. Hsp90 cochaperone Aha1 downregulation rescues misfolding of CFTR in cystic fibrosis. Cell. 2006; 127:803–815. [PubMed: 17110338]
163. Wei L, Xiao AY, Jin C, Yang A, Lu ZY, Yu SP. Effects of chloride and potassium channel blockers on apoptotic cell shrinkage and apoptosis in cortical neurons. Pflugers Arch. 2004; 448:325–334. [PubMed: 15057559]
164. Wong KR, Trezise AE, Crozatier B, Vandenberg JI. Loss of the normal epicardial to endocardial gradient of cftr mRNA expression in the hypertrophied rabbit left ventricle. Biochem Biophys Res Commun. 2000; 278:144–149. [PubMed: 11071866]
165. Wright J, Morales MM, Sousa-Menzes J, Ornellas D, Sipes J, Cui Y, Cui I, Hulamm P, Cebotaru V, Cebotaru L, Guggino WB, Guggino SE. Transcriptional adaptation to Clcn5 knockout in proximal tubules of mouse kidney. Physiol Genomics. 2008; 33:341–354. [PubMed: 18349385]
166. Xiang SY, Schegg K, Ye LL, Hatton WJ, Duan D. VDAC-1 may interact with CFTR to impart important cellular function in mouse heart. FASEB J. 2007; 21(726.3):A799.
167. Xiang SY, Ye LL, Hatton WJ, Duan D. ATPo-activated chloride channels play a key role in postconditioning-induced cardioprotection in mouse heart. FASEB J. 2008; 22 1130.10.
168. Xiong D, Heyman NS, Airey J, Zhang M, Singer CA, Rawat S, Ye L, Evans R, Burkin DJ, Tian H, McCloskey DT, Valencik M, Britton FC, Duan D, Hume JR. Cardiac-specific, inducible ClC-3 gene deletion eliminates native volume-sensitive chloride channels and produces myocardial hypertrophy in adult mice. J Mol Cell Cardiol. 2010; 48:211–219. [PubMed: 19615374]
169. Xiong D, Wang GX, Burkin DJ, Yamboliev IA, Singer CA, Rawat S, Scowen P, Evans R, Ye L, Hatton WJ, Tian H, Keller PS, McCloskey DT, Duan D, Hume JR. Cardiac-specific overexpression of the human short CLC-3 chloride channel isoform in mice. Clin Exp Pharmacol Physiol. 2009; 36:386–393. [PubMed: 18986326]
170. Xiong D, Ye L, Neveux I, Burkin DJ, Scowen P, Evans R, Valencik M, Duan D, Hume JR. Cardiac specific inactivation of ClC-3 gene reveals cardiac hypertrophy and compromised heart function. FASEB J. 2008; 22 970.25.
171. Xu Y, Dong PH, Zhang Z, Ahmmed GU, Chiamvimonvat N. Presence of a calcium-activated chloride current in mouse ventricular myocytes. Am J Physiol Heart Circ Physiol. 2002; 283:H302–H314. [PubMed: 12063303]

172. Yamamoto S, Ehara T. Acidic extracellular pH-activated outwardly rectifying chloride current in mammalian cardiac myocytes. Am J Physiol Heart Circ Physiol. 2006; 290:H1905–H1914. [PubMed: 16339831]
173. Yamamoto-Mizuma S, Wang GX, Hume JR. P2Y purinergic receptor regulation of CFTR chloride channels in mouse cardiac myocytes. J Physiol. 2004; 556:727–737. [PubMed: 14978203]
174. Yamamoto-Mizuma S, Wang GX, Liu LL, Schegg K, Hatton WJ, Duan D, Horowitz TL, Lamb FS, Hume JR. Altered properties of volume-sensitive osmolyte and anion channels (VSOACs) and membrane protein expression in cardiac and smooth muscle myocytes from Clcn3−/−mice. J Physiol. 2004; 557:439–456. [PubMed: 15020697]
175. Yang YD, Cho H, Koo JY, Tak MH, Cho Y, Shim WS, Park SP, Lee J, Lee B, Kim BM, Raouf R, Shin YK, Oh U. TMEM16A confers receptor-activated calcium-dependent chloride conductance. Nature. 2008; 455:1210–1215. [PubMed: 18724360]
176. Ye L, Dwyer L, Duan D. In vivo study of the role of cystic fibrosis transmembrane conductance regulator Cl^- channels in early and late ischemic preconditioning. Heart Disease. 2005; 4(362): 91.
177. Yin Z, Tong Y, Zhu H, Watsky MA. ClC-3 is required for LPA-activated Cl− current activity and fibroblast-to-myofibroblast differentiation. Am J Physiol Cell Physiol. 2008; 294:C535–C542. [PubMed: 18077605]
178. Zhang Z, Xu Y, Song H, Rodriguez J, Tuteja D, Namkung Y, Shin HS, Chiamvimonvat N. Functional roles of Cav1.3 ({alpha}1D) calcium channel in sinoatrial nodes: Insight gained using gene-targeted null mutant mice. Circ Res. 2002; 90:981–987. [PubMed: 12016264]
179. Zygmunt AC. Intracellular calcium activates a chloride current in canine ventricular myocytes. Am J Physiol. 1994; 267:H1984–H1995. [PubMed: 7977830]
180. Zygmunt AC, Gibbons WR. Calcium-activated chloride current in rabbit ventricular myocytes. Circ Res. 1991; 68:424–437. [PubMed: 1991347]
181. Zygmunt AC, Gibbons WR. Properties of the calcium-activated chloride current in heart. J Gen Physiol. 1992; 99:391–414. [PubMed: 1375275]

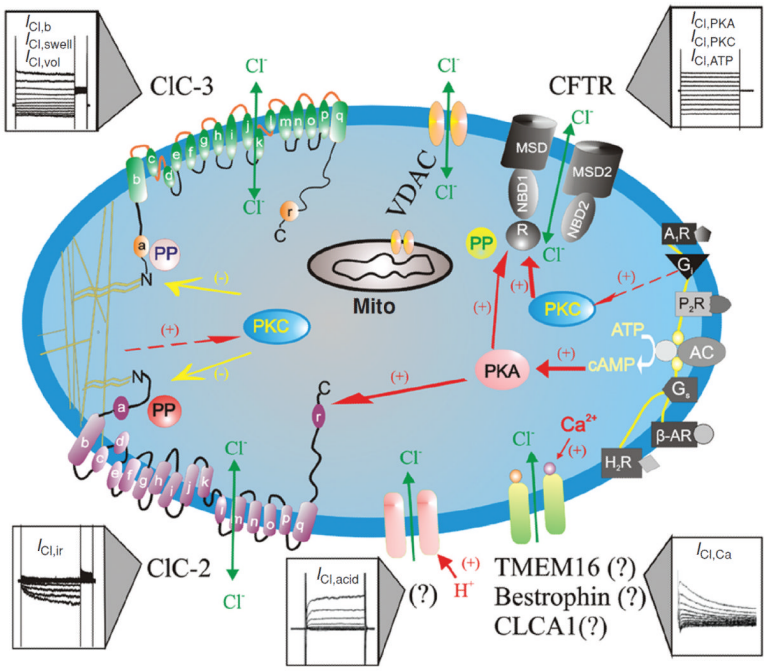

Figure 1.

Schematic representation of Cl^- channels in cardiac myocytes. Cl^- channels and their corresponding molecular entities or candidates are indicated. ClC-3, a member of voltage-gated ClC Cl^- channel family, encodes Cl^- channels that are volume-regulated ($I_{Cl,vol}$) and can be activated by cell swelling ($I_{Cl,swell}$) induced by exposure to hypotonic extracellular solutions or possibly membrane stretch. $I_{Cl,b}$ is a basally activated ClC-3 Cl^- current. ClC-2, a member of voltage-gated ClC Cl^- channel family, is responsible for a volume-regulated and hyperpolarization-activated inward rectifying Cl^- current ($I_{Cl,ir}$). Membrane topology models (α-helices a-r) for ClC-3 and ClC-2 are modified from Dutzler et al. (61). $I_{Cl,acid}$ is a Cl^- current regulated by extracellular pH and the molecular entity for $I_{Cl,acid}$ is currently unknown. $I_{Cl,Ca}$ is a Cl^- current activated by increased intracellular Ca^{2+} concentration ($[Ca^{2+}]_i$); Molecular candidates for $I_{Cl,Ca}$ include CLCA1, a member of a Ca^{2+}-sensitive Cl^- channel family (CLCA), bestrophin-2, a member of the Bestrophin gene family, and TMEM16, transmembrane protein 16. CFTR, cystic fibrosis transmembrane conductance regulator, encodes Cl^- channels activated by stimulation of cAMP-protein kinase A (PKA) pathway ($I_{Cl,PKA}$), protein kinase C (PKC) ($I_{Cl,PKC}$), or extracellular ATP through purinergic receptors ($I_{Cl,ATP}$). CFTR is composed by two membrane spanning domains (MSD1 and MSD2), two nucleotide-binding domains (NBD1 and NBD2), and a regulatory subunit (R). P, phosphorylation sites for PKA and PKC; PP, serine-threonine protein phosphatases; Gi, heterodimeric inhibitory G protein; A_1R, adenosine type 1 receptor; AC, adenylyl cyclase; H_2R, histamine type II receptor; Gs, heterodimeric stimulatory G protein; β-AR, β-adrenergic receptor; P_2R, purinergic type 2 receptor; proposed intracellular signaling pathway for purinergic activation of CFTR. VDAC, voltage-dependent anion channels (porin); mito, mitochondrion (48). (Copyright Request: Duan D. *J Physiol* 587: 2163–2177, 2009.)

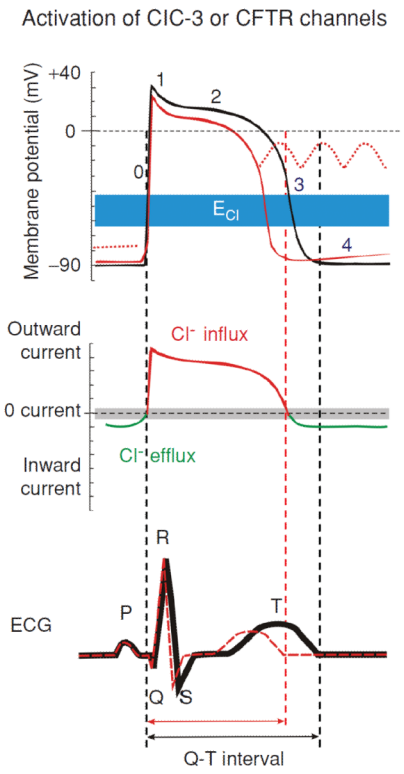

Figure 2.

Modulation of cardiac electrical activity by activation of Cl^- channels in heart. Changes in action potentials (*top*), membrane currents (*middle*), and ECG (*bottom*) due to activation of CFTR or volume-regulated ClC-3 Cl^- channels are depicted. *Top panel:* numbers illustrate conventional phases of a prototype ventricular action potential under control conditions (black) and after activation of I_{Cl} (red). Range of estimates for normal physiological values for Cl^- equilibrium potential (E_{Cl}) is indicated in blue. *Middle panel:* range of zero-current values corresponding to E_{Cl} is shown in grey. Activation of CFTR or ClC-3 channels generates both inward (indicated by green) and outward (indicated by red) currents and cause both depolarization as well as repolarization during the action potential. Activation of I_{Cl}, therefore, induces larger membrane depolarization and induction of early afterdepolarizations under conditions where resting K^+ conductance is reduced (dotted red lines in *top panel*). *Bottom panel:* the letters (P, Q, R, S, and T) indicate the conventional waves of electrocardiograph (ECG) complex under control conditions (black) and after activation of I_{Cl} (red). Corresponding to the shortening of action potential in ventricular myocytes activation of I_{Cl} causes a shortening of Q–T interval. See text for details (48). (Copyright Request: Duan D. *J Physiol* 587: 2163–2177, 2009.)

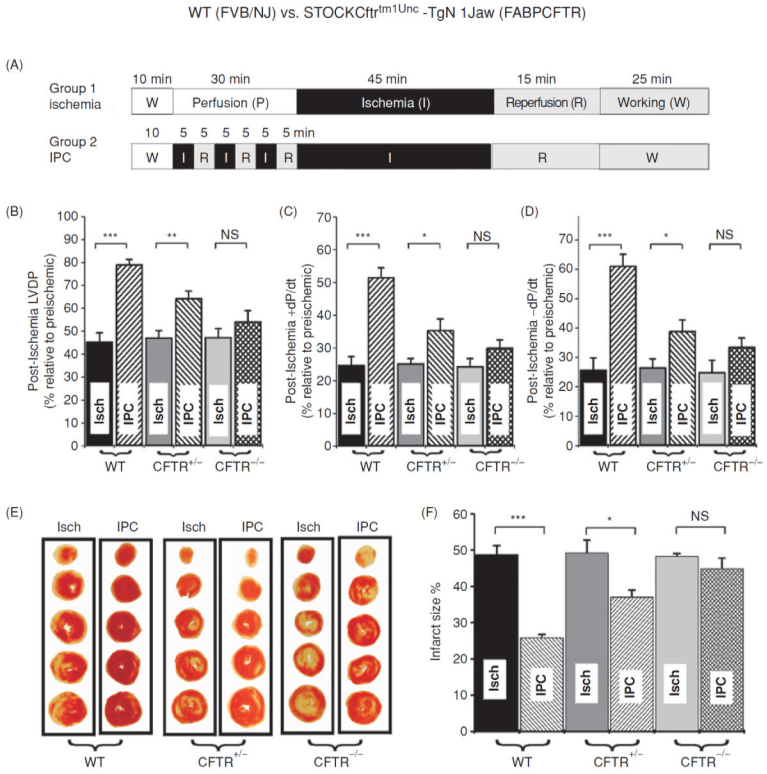

Figure 3.

Effects of *CFTR* gene knockout (FABPCFTR) on ischemic preconditioning in isolated working mouse heart. (A) Experimental protocol. (B–D) Recovery of left ventricular contractile (B and C.) and relaxation (D) function of wild-type WT (FVB/NJ), $CFTR^{+/-}$, and $CFTR^{-/-}$ (FABPCFTR) mice after 45 min ischemia and 40 min reperfusion. (E) IPC on infarct size of ventricles. Representative ventricle transverse slices after ischemia (Isch) or IPC. (F). Mean infarct size measured from age-matched WT, $CFTR^{+/-}$, or $CFTR^{-/-}$ mouse heart after ischemia or IPC ($n = 6$ for each group). *, $P < 0.05$; **, $P < 0.01$; ***, $P < 0.001$, *NS*: not significant (23). (Copyright Request: Chen H, et al. *Circulation* 110: 700–704, 2004.)

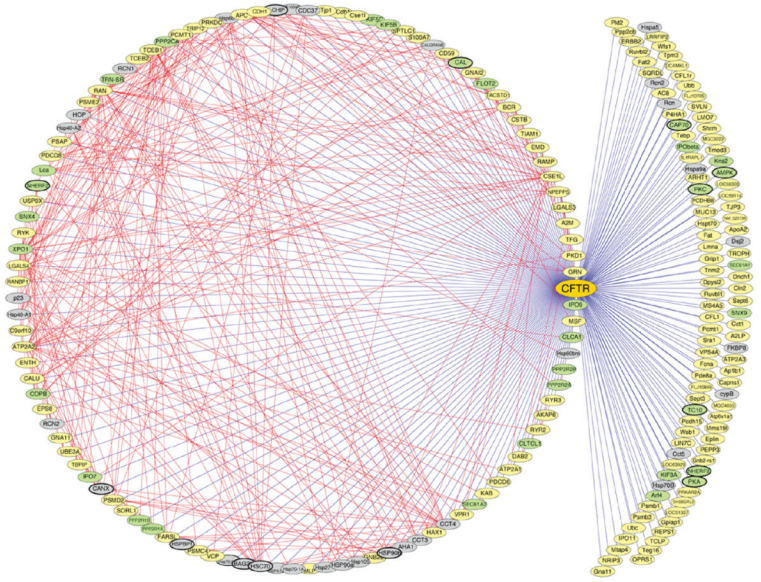

Figure 4.

The cystic fibrosis transmembrane conductance regulator (CFTR) interactome. All components comprising the CFTR interactome are depicted as nodes (ovals) in the network. Components identified in previous studies as CFTR interactors are highlighted with bold lines surrounding the ovals. Straight blue lines are edges in the network that show direct or indirect protein interactions between CFTR and the indicated component identified by MudPIT. Straight red lines illustrate edges that define interactions based on the BIND (http://www.bind.ca/Action) and DIP (http://dip.doe-mbi.ucla.edu/) protein interaction databases and the Tmm coexpression database (http://microarray.cpmc.columbia.edu/tmm/), which were accessed using the Cytoscape platform (http://www.cytoscape.org/). Proteins involved in folding and export from the ER are illustrated as gray nodes; green nodes highlight protein interactions involved in postendoplasmic reticulum trafficking and activity. Yellow nodes indicate interactors with unknown function. See the Supplementary Discussion for a more complete description of proteins defined by green and yellow nodes. The network includes proteins involved in the modulation of CFTR folding and function (162). (Copyright request: Wang et al. *Cell* 127: 803–815, 2006.)

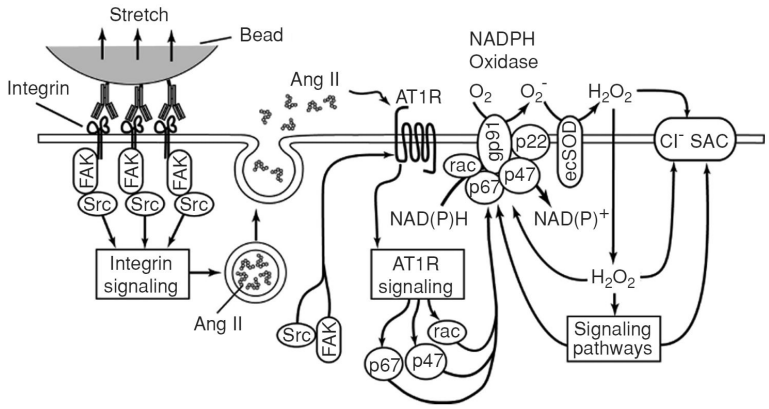

Figure 5.

Model of the mechanotransduction process coupling β1 integrin stretch to activation of Cl− channels in ventricular myocytes. Integrin stretch triggers the phosphorylation and activation of focal adhesion kinase and Src, and the release of angiotensin II (Ang II) from secretory vesicles. Ang II binds to the AT1 receptor (AT1R) and activates the AT1R signaling cascade. Components of the AT1R signaling cascade, possibly in concert with components of integrin signaling, induce the activation of p47*phox*, p67*phox*, and rac, which translocate to the membrane and assemble with gp91*phox* and p22*phox* to form the active NADPH oxidase complex. NADPH oxidase recruits NAD(P)H as an electron donor and catalyzes the transmembrane transfer of electrons to molecular O_2 to form superoxide (O_2^-). Extracellular O_2^- is rapidly converted to membrane-permeant H_2O_2 by ecSOD. H_2O_2 may activate Cl^- stretch-activated channels (SAC) either directly or via reactive oxygen species (ROS)-sensitive signaling pathways (18). (Copyright Request: Browe and Baumgarten. *J Gen Physiol* 124: 273–287, 2004.)

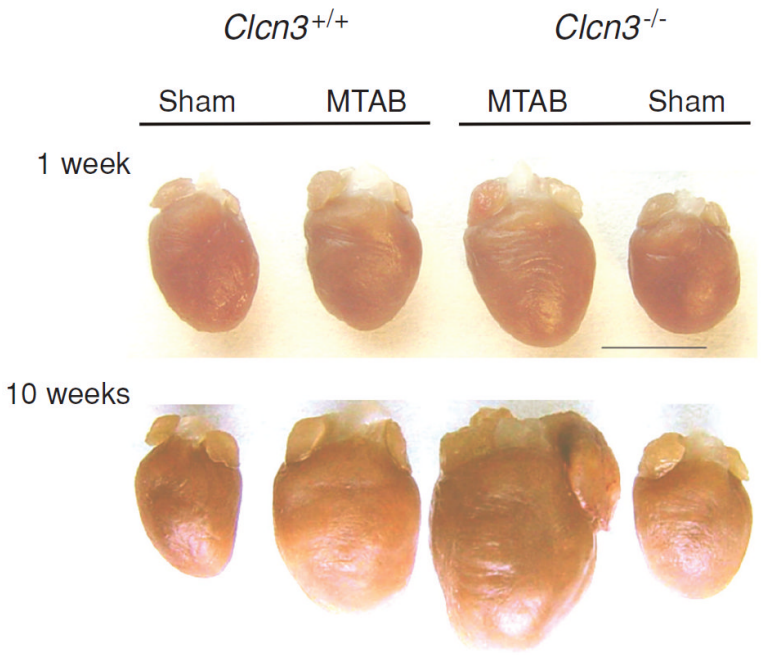

Figure 6.

Comparison of pressure overload-induced remodeling of wild-type and *Clcn3*$^{-/-}$ mouse hearts. Hearts from age-matched wild-type (WT, *Clcn3*$^{+/+}$) and *Clcn3*$^{-/-}$ mice were excised 1 week (*top panel*) or 10 weeks (*bottom panel*) after minimally invasive transverse aorta binding (MTAB) or sham operation are shown. Hearts were cleaned of blood and connective tissues and then fixed in 4% paraformaldehyde. Bar = 5 mm. Compared to WT mice disruption of *ClC-3* gene significantly changed the remodeling process after MTAB. Both left ventricle and atrium were extremely enlarged after 10 weeks of MTAB. [Adapted, with permission, from Duan (48)]. (Copyright Request: Duan D. *J Physiol* 587: 2163–2177, 2009)

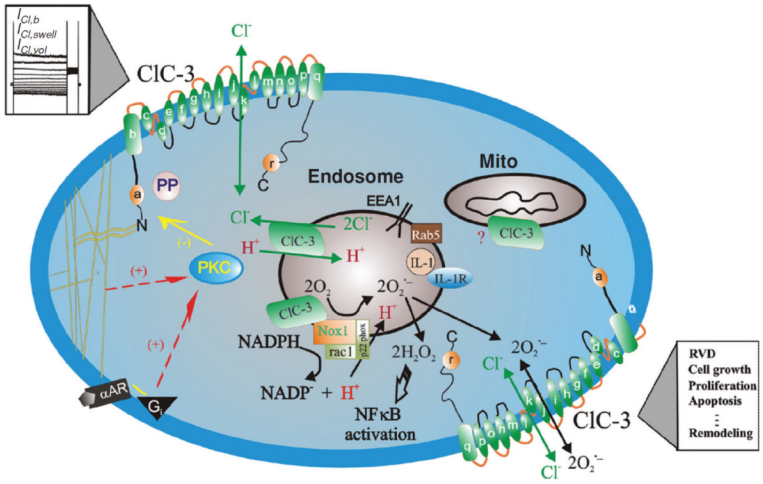

Figure 7.

Schematic representation of ClC-3 Cl^- channels in VSMCs. ClC-3, a member of voltage-gated ClC Cl^- channel family, encodes Cl^- channels in vascular smooth muscle cells that are volume regulated ($I_{Cl,vol}$) and can be activated by cell swelling ($I_{Cl,swell}$) induced by exposure to hypotonic extracellular solutions or possibly membrane stretch. $I_{Cl,b}$ is a basally activated ClC-3 Cl^- current. α-helices of ClC-3 are shown as a–r. ClC-3 proteins are expressed on both sarcolemmal membrane and intracellular organelles including mitochondria (mito) and endosomes. The proposed model of endosome ion flux and function of Nox1 and ClC-3 in the signaling endosome is adapted from Miller Jr. et al. (115). Binding of IL-1β or TNF-α to the cell membrane initiates endocytosis and formation of an early endosome (EEA1 and Rab5), which also contains NADPH oxidase subunits Nox1 and p22phox, in addition to ClC-3. Nox1 is electrogenic, moving electrons from intracellular NADPH through a redox chain within the enzyme into the endosome to reduce oxygen to superoxide. ClC-3 functions as a chloride-proton exchanger, required for charge neutralization of the electron flow generated by Nox1. The ROS generated by Nox1 result in NF-κB activation. Both ClC-3 and Nox1 are necessary for generation of endosomal reactive oxygen species (ROS) and subsequent NF-κB activation by IL-1β or TNF-α in VSMCs. Statins block ClC-3 channels, which causes hyperpolarization of the cell membrane, closure of Ca^{2+} channels and vasorelaxation, and inhibition of cell proliferation. PKC, protein kinase C; PP, serine-threonine protein phosphatases; α–AR, α-adrenergic receptor; Gi, heterodimeric inhibitory G protein. Nox: NADPH oxidase (59). (Copyright Request: Duan, Hypertension, 2010)

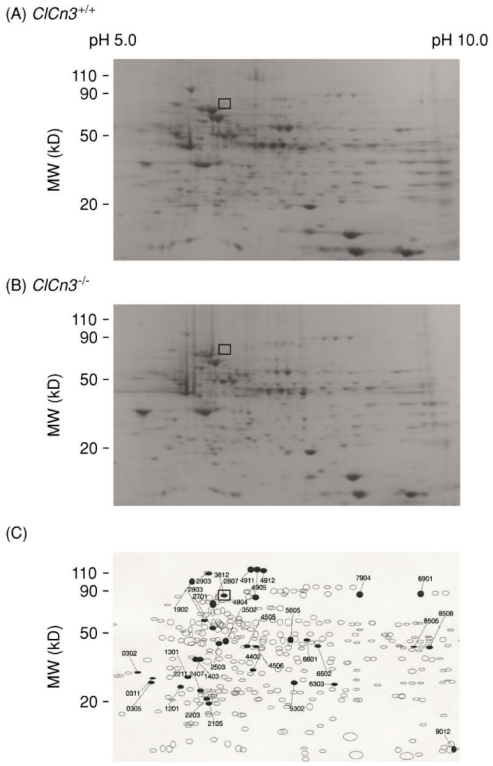

Figure 8.

Comparative two-dimensional (2D) electrophoresis analysis of protein expression patterns in membranes of cardiac cells from *Clcn3*$^{+/+}$ and *Clcn3*$^{-/-}$ mice. (A) representative 2D gel depicts Coomassie-stained proteins from wild-type (*Clcn3*$^{+/+}$) mouse heart. (B) Representative 2D gel depicts Coomassie-stained proteins from *Clcn3*$^{-/-}$ mouse heart. (C) Spot sets created from images of 2D gels of both wild-type and *Clcn3*$^{-/-}$ mouse heart run under the same conditions as the gels in A and B and compared using Bio-Rad PDQuest version 7.1.1 software. Three gels were run for each mouse heart type; two hearts were pooled to provide proteins for each gel. The filled symbols indicate changes in protein patterns in *Clcn3*$^{-/-}$ compared to wild type. A total of 35 proteins consistently changed (minimum criteria: more than twofold change) in membranes from *Clcn3*$^{-/-}$ mouse heart in all 3 experiments (6 missing proteins, 2 new proteins, 9 upregulated proteins, 15 downregulated proteins, and 2 translocated proteins). The open squares (□) in A, B, and C indicate the location (molecular mass 85 kDa and pI 6.9) of the ClC-3 protein spot (No. 3812) in the 2D gels, which was independently confirmed by Western blotting using a specific anti-ClC-3 C670~687 antibody (174). [Copyright Request: Yamamoto-Mizuma et al. (174) with permission from Blackwell Publishing].

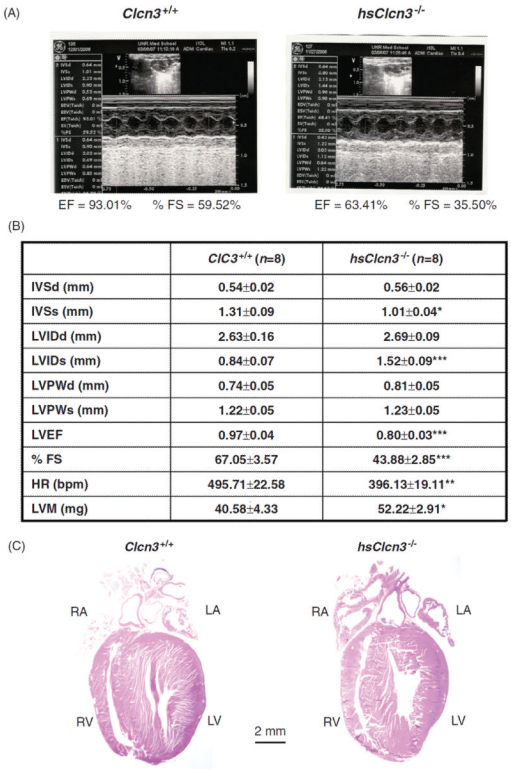

(B)

	ClC3$^{+/+}$ (*n*=8)	*hsClcn3*$^{-/-}$ (*n*=8)
IVSd (mm)	0.54±0.02	0.56±0.02
IVSs (mm)	1.31±0.09	1.01±0.04*
LVIDd (mm)	2.63±0.16	2.69±0.09
LVIDs (mm)	0.84±0.07	1.52±0.09***
LVPWd (mm)	0.74±0.05	0.81±0.05
LVPWs (mm)	1.22±0.05	1.23±0.05
LVEF	0.97±0.04	0.80±0.03***
% FS	67.05±3.57	43.88±2.85***
HR (bpm)	495.71±22.58	396.13±19.11**
LVM (mg)	40.58±4.33	52.22±2.91*

Figure 9.

Echocardiographic evaluation of cardiac function. (A) Representative M-mode echocardiography from wild-type (*Clcn3*$^{+/+}$; left) and heart-specific ClC-3 knockout (*hsClcn3*$^{-/-}$; right) mice. (B) Echocardiographic measurements in *Clcn3*$^{+/+}$ and *hsClcn3*$^{-/-}$ mice. IVSd, interventricular septum thickness at the end of diastole; LVDd, left ventricular (LV) dimension at the end of diastole; LVPWd, LV posterior wall thickness at the end of diastole; IVSs, interventricular septum thickness at the end of systole; LVDs, LV dimension at the end of systole; LVPWs, LV posterior wall thickness at the end of systole; LVEP, calculated LV ejection fraction; %FS, LV fractional shortening; estimated LV mass, LVM (mg) = 1.05[(IVS + LVID + LVPW)^3 − (LVID)^3], where 1.05 is the specific gravity of the myocardium. *, $P < 0.05$; **, $P < 0.01$; ***, $P < 0.001$ compared with *Clcn3*$^{+/+}$ mice. C. Single longitudinal section (μm) of hearts to demonstrate all four heart chambers. Longitudinal were stained with hematoxylin and eosin (Bar = 2 mm) (Duan D. et al. *unpublished data*.)

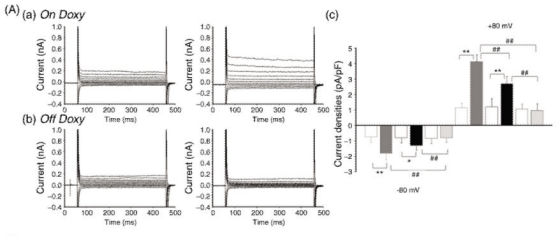

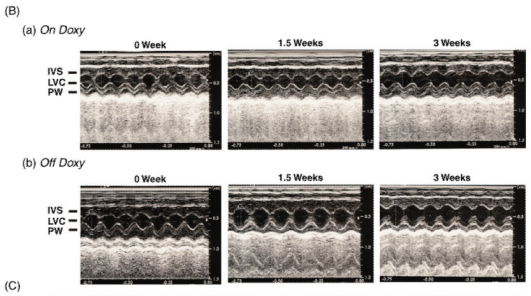

(C)

	0 week		1.5 weeks		3 weeks	
	On Doxy	Off Doxy	On Doxy	Off Doxy	On Doxy	Off Doxy
	n=8	*n*=15	*n*=4	*n*=12	*n*=5	*n*=9
IVSs (mm)	1.64±0.03	1.61±0.04	1.74±0.01	1.49±0.04*,##	1.58±0.03	1.48±0.04*
LVIDs (mm)	0.95±0.05	0.98±0.07	1.11±0.08	1.51±0.11***	1.19±0.05	1.57±0.11***,#
LVPWs (mm)	1.41±0.06	1.45±0.06	1.18±0.09	1.33±0.04	1.28±0.03	1.31±0.04
IVSd (mm)	0.81±0.02	0.81±0.02	0.76±0.02	0.76±0.02	0.79±0.02	0.80±0.02
LVIDd (mm)	2.66±0.18	2.93±0.08	2.70±0.09	3.26±0.12*,#	2.93±0.07	3.21±0.11*,#
LVPWd (mm)	1.08±0.05	1.08±0.03	0.99±0.04	1.08±0.04	0.99±0.05	1.07±0.05
FS (%)	64.13±1.70	67.10±1.78	59.28±1.90	54.34±1.87***	60.49±1.78	51.59±1.78***,##
LVEF (%)	95.11±0.66	95.95±1.58	93.02±0.94	89.83±1.22**	93.60±0.10	88.18±1.34**,##
Mass (mg/mm^2)	79.71±4.28	91.86±3.42	72.14±4.09	102.47±4.42##	87.76±5.34	102.14±3.01#
Body weight (g)	34.86±2.55	43.10±1.87#	33.15±3.61	41.21±2.08	38.22±1.84	36.34±2.40
Mass/BW Ratio	2.40±0.22	2.16±0.08	2.29±0.23	2.54±0.14*	2.30±0.08	2.87±0.14***,#

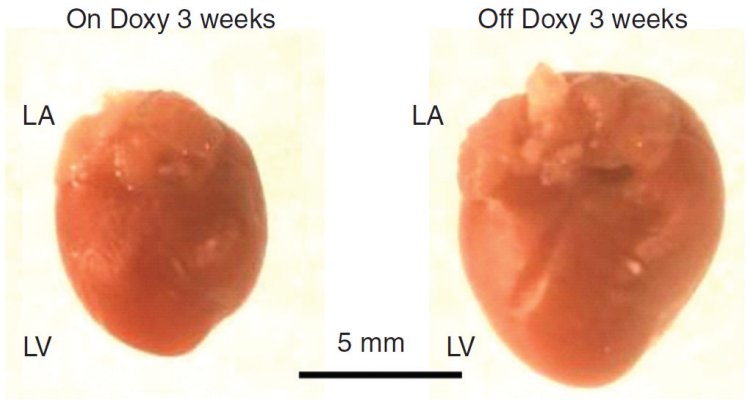

Figure 10.

Effects of inducible heart-specific ClC-3 knockout on cardiac volume-regulated Cl^- current (VRCC) and heart function. (A) Representative current traces in isotonic condition and under hypotonic challenge recorded in freshly isolated atrial myocytes from the inducible heart-specific ClC-3 knockout (*doxyhsClC-3*$^{-/-}$) mice with doxycycline (*on Doxy*) in the diet (panel a), or after withdraw of doxycycline (*off Doxy*) from the diet for 3 weeks (panel b). (c) Summary of VRCC current densities in isotonic and hypotonic solutions, recorded at +80 mV and −80 mV. (B) Representative M-mode echocardiography from on Doxy (a) and off Doxy (b) mice. (C) Time-dependent changes in M-mode echocardiogram of age matched *on Doxy* or *off Doxy* for 1.5 and 3 weeks. *, $P < 0.05$; **, $P < 0.01$; ***, $P < 0.001$ versus *off Doxy* 0 week;$^{\#}$, $P < 0.05$;$^{\#\#}$, $P < 0.01$;$^{\#\#\#}$, $P < 0.001$ versus *on Doxy* at the same time point. (D) Comparison of hearts isolated from age-matched (11-week old) *doxyhsClcn3*$^{-/-}$ mice *on Doxy or off Doxy* for 3 weeks. Hearts were cleaned up blood and connective tissues and fixed in 4% paraformaldehyde. [Adapted, with permission, from Xiong et al. (168).]

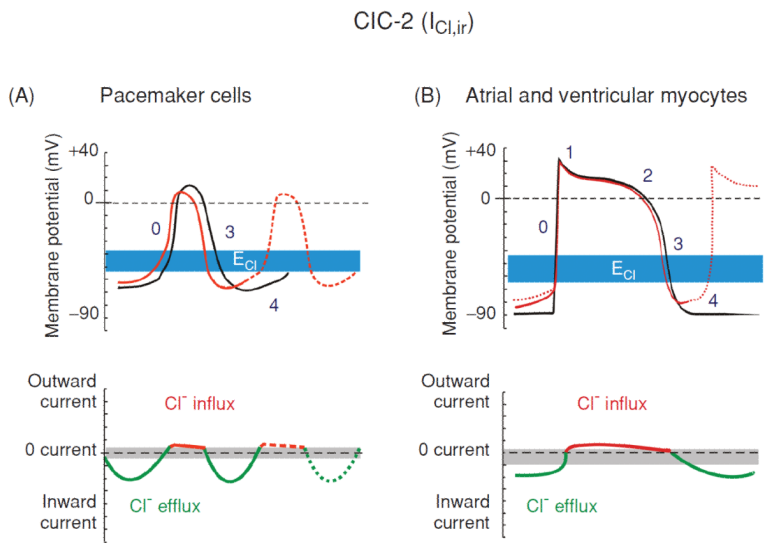

Figure 11.

Modulation of cardiac electrical activity by activation of ClC-2 channels in cardiac pacemaker cells and myocytes. Changes in action potentials (*top panels*) and membrane currents (*bottom panels*) of cardiac pacemaker cells (A) or atrial and ventricular myocytes (B) due to activation of ClC-2 channels are depicted. $I_{Cl,ir}$ is activated by hyperpolarization, cell swelling, and acidosis. *Top panels:* numbers illustrate conventional phases of a prototype ventricular action potential under control conditions (black) and after activation of I_{Cl} (red). Range of estimates for normal physiological values for Cl^- equilibrium potential (E_{Cl}) is indicated in blue. *Bottom panels:* range of zero-current values corresponding to E_{Cl} is shown in grey. (A) Activation of $I_{Cl,ir}$ in pacemaker cells during hyperpolarization causes acceleration of phase 4 depolarization and automaticity, shortening of action potential duration, and decrease in cycle length and action potential amplitude (dashed red line in *top panel*). (B) Activation of $I_{Cl,ir}$ in atrial and ventricular myocytes during hyperpolarization causes depolarization of resting membrane potential and induction of phase 4 auto depolarization and abnormal electrical impulse (trigger activity) and automaticity (dotted red line in *top panel*). [Adapted, with permission, from Duan (48)]. (Copyright Request: Duan D. *J Physiol* 587: 2163-2177, 2009)

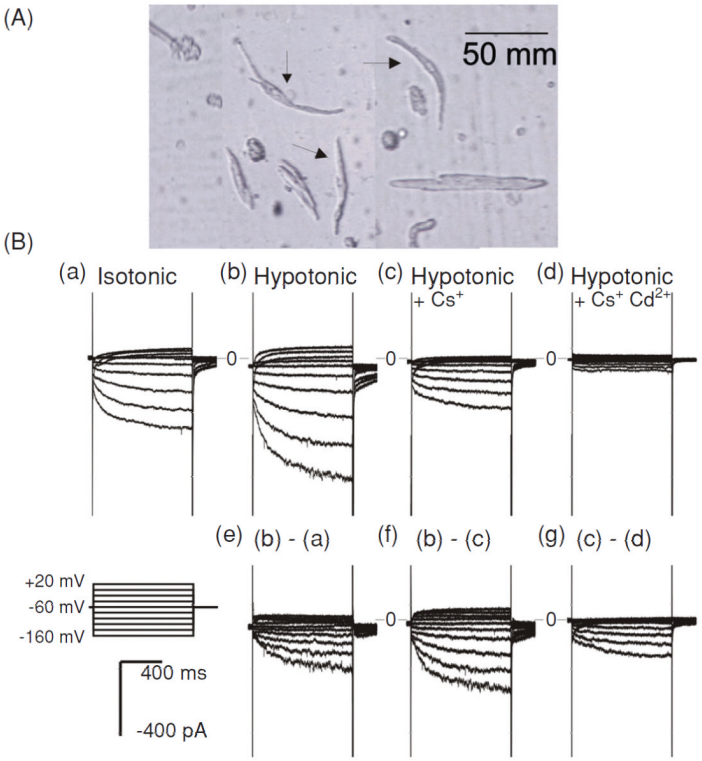

Figure 12.

Whole-cell currents recorded from SAN cells of guinea-pig heart. (A) An example of single SAN cells (arrows) isolated from the SAN region of guinea pig heart by enzymatic dispersion. (B) Whole-cell currents recorded from SAN cells. When cations (Na^+ and K^+) were included in the extracellular solutions, inward currents were slowly activated upon hyperpolarization under isotonic (a) conditions. Exposure of the same cell to hypotonic extracellular solution caused cell swelling and an increase in the inward current amplitude (b). The difference current caused by hypotonic cell swelling is shown in panel e. Subsequent replacement of 20 mmol/L of NaCl with CsCl caused a significant inhibition of the inward current (c). The Cs^+-sensitive current is shown in panel f. Subsequent addition of 0.2 mmol/L of Cd^{2+} to the hypotonic solution caused an inhibition of the inward current (d). The Cd^{2+}-sensitive currents are shown in panel g (89).

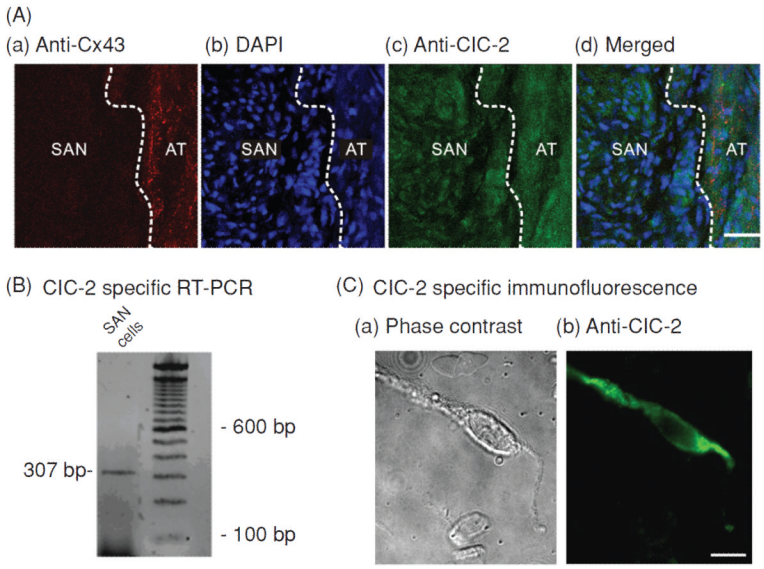

Figure 13.

Molecular expression of *ClC-2* in SAN cells. (A) Localization of *ClC-2* chloride channels in guinea-pig SAN tissue. (a) Section labeled with anti-Connexin 43 (red) to illustrate the adjacent atrial (AT) septum was positively labeled while the SAN was negative (dark region), which clearly delineates the SAN region from the AT septum (dashed white line). (b) Section stained with 4′,6-diamidino-2-phenylindole (DAPI) (blue) to compare nuclei density in the SAN region and in AT. The SAN region had a higher DAPI staining density (higher nuclei density) than the adjacent AT. (c) Section stained with anti-*ClC-2* (green). ClC-2 immunoreactivity is evident in both SAN and AT regions. (d) Merged images of a, b, and c illustrate that *ClC-2* is expressed in the densely nucleated and Cx43 negative SAN region. (B) Agarose gel depicting real time polymerase chain reaction product of *ClC-2* amplified from mRNA prepared from enzymatically dispersed guinea-pig SA nodal cells. (C) Images of ClC-2-like immunofluorescence in a representative SAN cell visualized using fluorescent microscopy. Phase contrast (a) and fluorescent micrographs (b) of a single SAN cell.

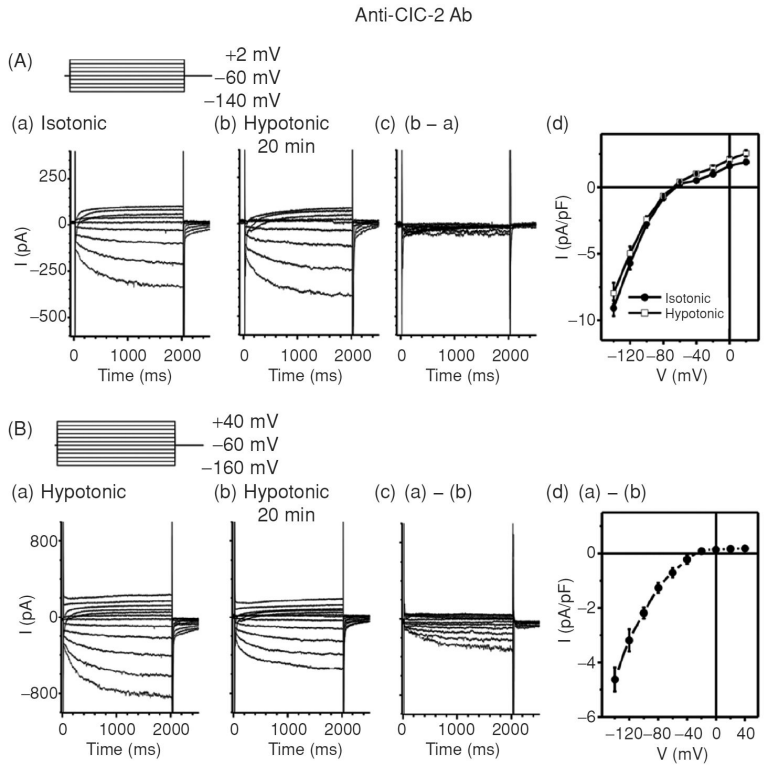

Figure 14.

Effects of Anti-*ClC-2* Ab on $I_{Cl,ir}$ in SAN cells. (A) Representative whole-cell currents recorded from SAN cells under isotonic (panel a) and hypotonic (panel b) conditions in the presence of anti-ClC-2 Ab in the pipette solutions. SAN cells were exposed to isotonic solution for at least 10 min before whole-cell recordings. Currents shown in panel a were recorded right after successful whole-cell configuration under isotonic conditions. Currents shown in panel b were recorded after exposure to hypotonic solution for 20 min. Pipette and bath solutions were identical to those described in Figure 1B except the pipette solution contained 3 μg/mL anti-ClC-2 Ab. (d) Mean *I–V* from 5 SAN cells under the same conditions. (B) SAN cells were exposed to hypotonic solution for 20 min to fully activate $I_{Cl,ir}$ before whole-cell recordings. Bath and pipette solutions were the same as in panel A. Representative current traces recorded by voltage-clamp (protocol is shown in inset) from the SAN cell immediately after membrane rupture (a) and after 20 min of anti-ClC-2 Ab dialysis (b). The anti-ClC-2 Ab-sensitive current (a)–(b) is shown in (c) (current traces) and (d) (mean *I–V*, $n = 5$). Notice the anti-ClC-2 Ab-sensitive current (c) was similar to $I_{Cl,ir}$ shown in Figure 1 and the typical I_{Ca} and I_f (b) were not affected by anti-ClC-2 Ab.

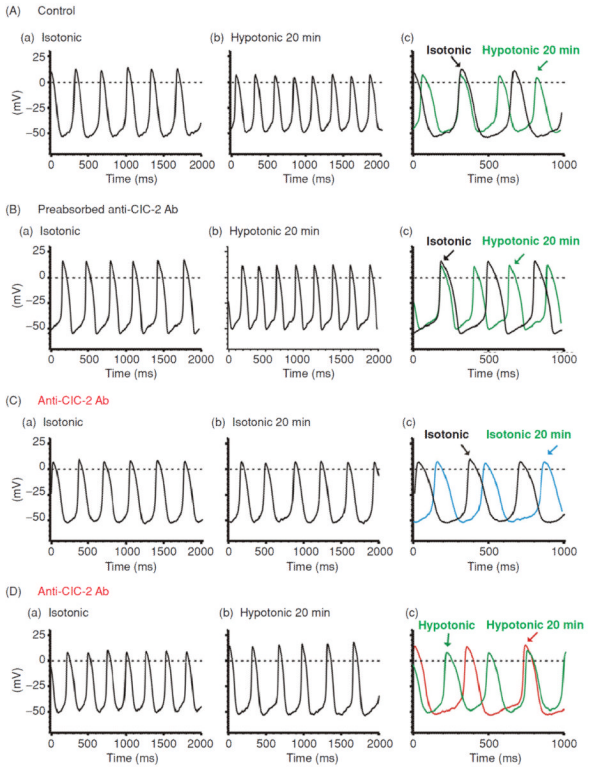

Figure 15.

Effects of Anti-*ClC-2* Ab on pacemaker action potential in SAN cells. (A) Representative spontaneous action potentials recorded from an SAN cell by current-clamp (no current injection) with pipette solution containing no anti-*ClC-2* Ab under isotonic (a) and hypotonic (b) conditions. SAN cells were exposed to isotonic solution for at least 10 min before action potential recordings. Action potentials shown in panel a were recorded right after successful whole-cell configuration under isotonic conditions. Action potentials shown in panel b were recorded after exposure to hypotonic solution for 20 min. For comparison, the action potentials recorded under these conditions were superimposed with an expanded time scale in panel **c**. The dotted lines indicate zero voltage. (B) Spontaneous action potentials recorded from a SAN cell by current clamp using a pipette solution containing pre-absorbed anti-*ClC-2* Ab (control) and cell was exposed to isotonic solutions for 10 min (a) and hypotonic solutions for 20 min (b). For comparison, the action potentials recorded under these conditions were superimposed with an expanded time scale in panel c. (C) SAN cells were perfused with isotonic solutions for 20 min before whole-cell recordings. Action potentials were recorded immediately after membrane rupture (a) and after dialysis of anti-*ClC-2* Ab for 20 min (b) under the same isotonic conditions. Panel c shows the expanded and superimposed action potentials as shown in panel a and panel b. Note that after 20 min dialysis of anti-*ClC-2* Ab in to the cell the spontaneous action potential rate was not significantly altered. (D) SAN cells were exposed to hypotonic solution for 20 min to fully activate $I_{Cl,ir}$ before whole-cell recordings. Action potentials were recorded immediately after membrane rupture (a) and after dialysis of anti-*ClC-2* Ab for 20 min (b). Panel c shows the expanded and superimposed action potentials as shown in panel a and panel b. Note that the spontaneous action potential rate significantly decreased after 20 min dialysis of anti-*ClC-2* Ab in to the cell, which corresponds with the decrease in inward

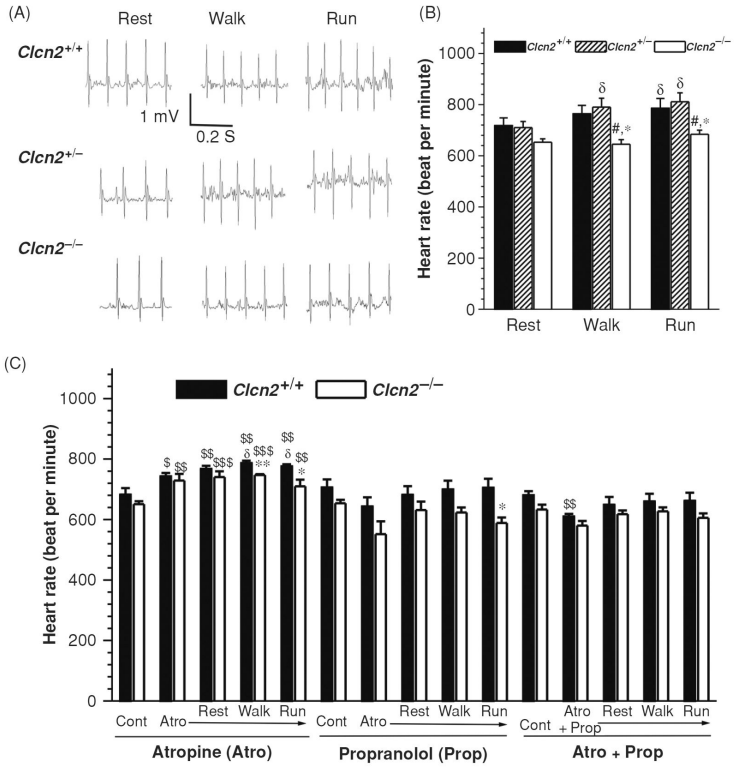

Figure 16.

Telemetry electrocardiogram (ECG) recordings in *Clcn2*$^{-/-}$ mice and their *Clcn2*$^{+/+}$ and *Clcn2*$^{+/-}$ littermates during treadmill exercises. (A) Representative ECG (Lead II) recordings in *Clcn2*$^{+/+}$, *Clcn2*$^{+/-}$, and *Clcn2*$^{-/-}$ mice while they were subjected to treadmill exercise at (a) rest period: acclimation at 0 m/min, incline 0° for 5 min; (b) walk period: walking at 5m/min, incline 0° for 5 min; (c) run period: running at 15 m/min, uphill incline 8° for 5 min. (B) Mean heart rate during the last minute of each treadmill exercise segment for the *Clcn2*$^{+/+}$ (n = 6), *Clcn2*$^{+/-}$ (n = 5), and *Clcn2*$^{-/-}$ (n = 7) mice. (C) Mean heart rate of the *Clcn2*$^{+/+}$ (n = 5) and *Clcn2*$^{-/-}$ (n = 4) mice before (Control, Cont) and after the intraperitoneal injection of atropine (Atro), propranolol (Prop), or atropine plus propranolol (Atro + Prop) during the last minute of each treadmill exercise segment (rest, walk, and run). *, $P < 0.05$; **, $P < 0.01$; ***, $P < 0.001$ versus *Clcn2*$^{+/+}$; $^{\#}$, $P < 0.05$; $^{\#\#}$, $P < 0.01$; $^{\#\#\#}$, $P < 0.001$ versus *Clcn2*$^{+/-}$; $^{\$}$, $P < 0.05$; $^{\$\$}$, $P < 0.01$; $^{\$\$\$}$, $P < 0.001$ versus control (Cont); ^{d}, $P < 0.05$ versus rest (89).

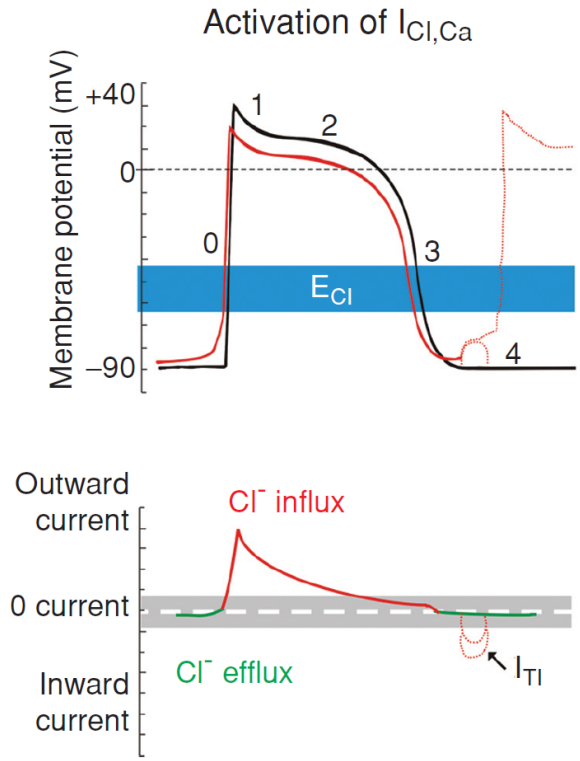

Figure 17.
Modulation of cardiac electrical activity by activation of Ca^{2+}-activated Cl^- channels in heart. Changes in action potentials (*top*) and membrane currents (*bottom*) due to activation of Ca^{2+}-activated Cl^- channels are depicted. *Top panel:* numbers illustrate conventional phases of a prototype ventricular action potential under control conditions (black) and after activation of I_{Cl} (red). Range of estimates for normal physiological values for E_{Cl} is indicated in blue. *Bottom panel:* Range of zero-current values corresponding to E_{Cl} is shown in grey. Activation of $I_{Cl,Ca}$ during $[Ca^{2+}]i$ overload results in oscillatory transient inward current (I_{TI}) and induction of delayed afterdepolarization (DAD) (dotted red lines). [Adapted, with permission, from Duan (48)]. (Copyright Request: Duan D. *J Physiol* 587: 2163-2177, 2009.)